# Chapter - 3
# Apremilast loaded solid lipid nanocarriers

## 3. Introduction

As discussed above, the systemic administration of Apremilast is associated with adverse effects (nausea, diarrhoea, upper respiratory infections, urinary tract infection, depression, suicidal tendencies, and weight loss) [1,2]. It was reported that the psoriasis patient's dermis exhibit upregulated expression of mRNA and protein levels of PDE4 and its isoforms [3]. In such cases, the topical delivery of Apremilast can show better therapeutic efficacy over oral delivery with minimal systemic adverse effects [4]. However, with conventional topical formulations (ointment, cream, and gels), the skin acts as a barrier and restricts the drug's permeation [5]. Hence, conventional topical therapies need a high drug dose for optimum concentration in the skin layers, which leads to irritation on the skin.

To overcome the limitations of conventional therapies, nanocarriers-based drug delivery systems have attracted great interest in recent days. Moreover, in psoriasis conditions, the plaques formation, dry skin, and hyperproliferation of keratinocytes may limit the drug permeation. Nanocarriers-based topical delivery may improve permeation, patient compliance and prolong the drug release in skin layers and protect the drug from degradation [5].

Among lipid nanocarriers, SLNs exhibit high drug loading capacity and controlled release compared to other colloidal carriers (liposomes and emulsion systems). The lipids used in the preparation of SLNs are inexpensive compared to the lipids used in the preparation of liposomes [6,7]. The nanosize of the SLNs forms a thin layer over the stratum corneum and prevents water evaporation, which ultimately reduces TEWL, increases moisture level, and hydrates the skin. The hydration leads to gaps in the corneocytes and favors accumulation (embedding) of SLNs in the stratum corneum. The particles embedded in stratum corneum layers favors skin retention, release the drug at a slower rate, and exhibit prolonged action with minimal or no systemic absorption [8].

### 3.1. Materials

Acetonitrile, methanol (HPLC grade), propylparaben, methylparaben, orthophosphoric acid, and potassium dihydrogen phosphate were procured from Merck, Mumbai, India. Precirol ATO 5 (glyceryl palmitostearate), Compritol 888 ATO (glyceryl dibehenate) were obtained as gift samples from Gattefosse, India. Stearic acid, Glyceryl monostearate, and Oleic acid were purchased from Central Drug House (P) Ltd fine chemicals (New Delhi, India). Dynasan 114 (trimyristin) was acquired from Sasol Olefins & Surfactants (Germany). Polysorbate 80 was acquired from S.D. Fine Chemicals (India). Kolliphor CS12, Carbopol® 974P N.F, and Lutrol® F 127 (Poloxamer 407) were received as a gift sample from Lubrizol (Belgium) and BASF (India), respectively. Antibiotic-antimycotic solution and Dulbecco's modified Eagle's medium (DMEM) were obtained from Thermofisher Scientific (India). Fetal bovine serum was purchased from Himedia (Mumbai, India). Cellophane tape was purchased from Scotch 3 M, USA. All other solvents, reagents, and chemicals used were of analytical grade.

### 3.2. Methods

#### 3.2.1. Selection of solid lipid and surfactant

Solid lipid selection was made by the visual observation method. A fixed amount of Apremilast (2 mg) was taken in clear glass vials and placed in the water shaker bath at 80 ± 5 ºC. Pre-weighed solid lipids (Glyceryl monostearate, Compritol 888 ATO, Precirol ATO 5, Stearic acid, Dynasan 114) were added in small increments till the formation of a clear lipid solution. The maximum amount of the lipids required to solubilize the 2 mg of Apremilast was estimated visually. The surfactant selection was performed based on emulsification ability; by assessing the size, PDI, and entrapment efficiency. The surfactant selected should be within the required hydrophilic-lipophilic balance (RHLB) value to obtain a small particle size. For selecting appropriate surfactant, SLNs formulations were prepared by hot emulsification using

surfactants with different HLB values in the range of 12-20. The screened surfactants were Kolliphor CS 12 (HLB 12), polysorbate 80 (HLB 16), and poloxamer F 127 (HLB 20). All the experiments were performed in triplicates.

### 3.2.2. Drug excipient compatibility study and solution stability study in release media

The excipient compatibility study of Apremilast with excipients was assessed by visual inspection and change in the percent assay of the drug using HPLC method. The study was performed by mixing individual excipient and drug at a 1:1 ratio. To the mixture, 100 µL milli-Q water was added and stored at 30 ºC for 3 months. The solution stability study of Apremilast with release media (Phosphate buffer saline (pH 7.4) with 0.15% sodium lauryl sulfate) was assessed by change in the percent assay of the Apremilast for 48 h.

### 3.2.3. Quality by design approach

The QbD approach minimizes the complications associated with nanoformulation optimization. QbD helps in the assessment of material and process variable factors involved in product optimization and enhances the process capability with minimum product variability [9].

#### 3.2.3.1. Identification of quality target product profile and critical quality attributes

The quality target product profile (QTPP) provides an extensive summary of the desired product requirements to exhibit maximum safety and efficacy. Before implementing the QbD approach, the QTPP setup was established, comprising the various factors affecting permeation of the Apremilast by SLNs loaded gel for topical delivery. Critical quality attributes (CQAs) are selected to meet QTTP, which controls the desired characteristic features of the finished target product. The CQAs of the finished product should impart the quality required to complete the patient's needs. Thus, before optimizing Apremilast loaded SLNs, the QTPP and

CQAs were selected utilizing existing literature and prior knowledge in developing lipid-based systems [9].

#### 3.2.3.2. A risk assessment by Ishikawa diagram

The Ishikawa diagram was used to screen the critical formulation and process variables for Apremilast SLNs formulation. The risk-based matrix assessment was performed based on the potential challenges affecting the formulation attributes. The low, medium and high-level risk potential factors were utilized to select the critical material attributes (CMAs) and critical process parameters (CPPs) using the risk estimation matrix. Each of the chosen factors was evaluated for the probability of occurrence, severity, and detectability to execute failure mode evaluation and analysis (FMEA). Using equation 3.1, the risk priority number was calculated with the rank order of 0 to 5. The obtained RPN score was considered for screening and optimizing the critical material attributes and critical process parameters [10].

$$\mathrm{RPN} = \mathrm{Ocucrrence\,(O)} \times \mathrm{Severity\,(S)} \times \mathrm{Detectability\,(D)} \qquad \text{(Eq. 3.1)}$$

#### 3.2.3.3. Optimization of Apremilast loaded SLNs utilizing experimental design

To optimize the formulation, a design of experiments was employed to determine the effects of multiple factors concurrently. It minimizes the number of trials and overcomes the drawbacks of one variable or one factor at a time.

Various mathematical models of response surface methodology like factorial design, Box-Behnken design, Central Composite Design (CCD) are used, which exhibit different assets and traits. Among the various response surface methodology (RSM) techniques, Box–Behnken design (BBD) allows a three-factor, three-level statistical screening approach to evaluate the main as well as interaction effects of the formulation variables and process parameter on

measured responses of prepared SLNs to optimize the formulation with the minimum number of experiments [9,11].

### 3.2.4. Preparation and optimization of SLNs

SLNs based formulation was prepared by hot emulsification followed by size reduction using probe sonication. Here the lipid and aqueous phases were prepared separately. In brief, the lipid phase consists of a batch quantity of solid lipid, preservative agents (methylparaben and propylparaben), and Apremilast. The Apremilast was dissolved in acetone for the uniform distribution in the lipid. The mixture was subjected to heating at 70 ± 2 °C for 30 min under continuous stirring to evaporate the acetone. The acetone belongs to the class 3 residual solvents, which have minimum toxicity; moreover, the low boiling point aids in easy evaporation. The surfactant solution was prepared in milli-Q water and it was pre-heated to 70 ± 2 °C separately. The pre-heated aqueous phase was transferred to the melted lipid mixture and mixed for 20 min to form a homogeneous mixture. Then the obtained mixture was subjected to sonication and cooled to room temperature for solidification of nanosized particles. Further, the dispersion was centrifuged at 5000 rpm for 5 min. The supernatant lipid nanocarriers dispersion was subjected to ultracentrifugation at 35,000 rpm to separate the SLNs from dispersion. The supernatant was separated, and the settled nanocarriers were redispersed in milli-Q water.

### 3.2.5. Scale-Up studies of the optimized formulation

Based on the validation parameters, the selected batch was scaled up to 50 mL and 100 mL. In scale-up, quantities required for formulation (composition) were increased proportionally. Initially, 10 mL batches were performed for optimization. In the case of 50 mL and 100 mL batch, vessel diameter and the probe sonicator diameter were varied in comparison to the 10 mL batch. The probe sonicator with a 3 mm tip diameter (capacity 1-10 mL) was used to

prepare a batch size with 10 mL. The probe sonicator with a 13 mm tip diameter (capacity 10-250 mL) was used to prepare the batch size with 50 mL and 100 mL.

### 3.2.6. Characterization of Apremilast loaded SLNs

#### 3.2.6.1. Attenuated total reflection-Fourier transform infrared spectroscopy (ATR-FTIR)

The prepared Apremilast SLNs formulation was evaluated to differentiate possible interactions between drugs and excipients. The Apremilast SLNs formulation, physical mixture, and pure Apremilast spectrum were recorded using an attenuated total reflectance Fourier transform infrared (ATR-FTIR) spectroscopy (Bruker, USA). The spectra generated was scanned over 4000 to 400 $cm^{-1}$ at a resolution of 1 $cm^{-1}$ and averaged over 100 scans. The data generated were compared to determine the feasibility of chemical compatibility amid SLNs and Apremilast [12].

#### 3.2.6.2. Particle size, zeta potential and morphology

Lipid nanocarriers loaded with the drug were evaluated for their mean particle size, poly dispersibility index (PDI), and zeta potential by dynamic light scattering technique at 173° backscattering and 25 ℃ temperature with dispersant refractive index 1.330 using Zeta Sizer (Nano ZS, Malvern Instruments, UK). The aliquot of lipid nanocarriers dispersion was diluted 10 times with Milli-Q water. The zeta potential was assessed based on electrophoretic mobility under an electric field at 25 ºC using ultrapure water as a diluting medium. The prepared dispersion morphology was measured using Field Emission Scanning Electron Microscopy (FESEM) (Apreo Switch XT microscope). The nanocarrier dispersion was diluted with Milli-Q water and spread on the coverslip. The dispersion was subjected to drying in a vacuum and sputtering before performing morphological studies [13].

### 3.2.6.3. Entrapment Efficiency

The % entrapment efficiency of the encapsulated or dispersed drug was determined using the direct method. The formulation was centrifuged at 5000 rpm for 5 min, and the supernatant lipid nanocarriers dispersion was subjected to ultracentrifugation at 35,000 rpm to separate the SLNs from dispersion. The supernatant was separated, and the settled nanocarriers were subjected to lysis and extraction using an Acetonitrile and centrifuged to separate solid lipid. The obtained solution was filtered and analyzed, utilizing the validated HPLC method at 229 nm. The percent entrapment efficiency was calculated using equation 3.2 [8].

$$\%\ \text{Entrapment efficiency} = \frac{\text{Amount of drug in lipid nanocarriers}}{\text{Total amount of drug taken}} \times 100 \qquad \text{(Eq. 3.2)}$$

### 3.2.6.4. In-vitro drug release studies of SLNs dispersion

In-vitro drug release studies were conducted for selected SLNs dispersion (10 mL, 50 mL, and 100 mL) and the free drug solution using the dialysis bag method. SLNs dispersion and free drug solution equivalent to 0.5 mg of Apremilast were taken in regenerated seamless cellulose membrane (Himedia, molecular weight cut off 12,000 - 14,000 Da). Phosphate buffer saline (pH 7.4) with 0.15% sodium lauryl sulfate was used as release media to maintain sink conditions (selected based on USP monograph). The dialysis bag was closed at both ends and immersed in 15 mL of release medium. The buffer was sonicated for 30 min before the study's initiation to avoid foam formation and interference of air bubbles. At each time interval, 1 mL of aliquots was withdrawn and replaced with an equal volume of fresh release medium to maintain sink condition. The amount of drug released was estimated in the aliquots using the validated HPLC technique. The obtained data were assessed by fitting the discerned values into different model equations, and a best-fit release model was found using "DDSolver," excel add-in [14].

### 3.2.6.5. Cytotoxicity study

MTT assay was utilized to reveal in-vitro cytotoxicity of free Apremilast dispersion and Apremilast loaded SLNs dispersion in HaCaT (Human Keratinocyte) cell lines. HaCaT cell lines were cultured in 96-well plates containing Dulbecco's modified eagle's medium (DMEM) supplemented with 10% fetal bovine serum (FBS) and antibiotics at 37 °C under 5% $CO_2$ ($2\times10^4$ cells/well). After 24 h, cells were imperiled with various concentrations of free Apremilast and Apremilast-loaded SLNs dispersion (0-10000 µM). The cells were incubated for 72 h, and cytotoxicity was estimated by MTT dye (1 mg/mL). The absorbance was monitored at 570 nm and 630 nm using Synergy HT multi- detection microplate reader (Biotek, Winooski, VT) [8].

### 3.2.6.6. Cell uptake study using Coumarin-6

The Coumarin-6 loaded SLNs formulation was prepared by the optimized method (similar to optimized Apremilast loaded SLNs preparation). The intracellular uptake study of Coumarin-6 dispersion and Coumarin-6 SLNs was performed by exploring the intrinsic fluorescence property of Coumarin-6 using a fluorescence microscope (Zeiss Vert.A1). Briefly, HaCaT cells ($1 \times 10^5$/well) were grown on the coverslips in 6 well plates and incubated for 24 h at 37 °C in the $CO_2$ incubator. Further, cells were incubated with Coumarin-6 dispersion, and Coumarin-6 loaded SLNs at 1 µg/mL concentration. After 1 and 3 h of incubation, the cells were washed with phosphate buffer saline and fixed with 4% paraformaldehyde for 10 min. The cells were further permeabilized with 0.1% Triton-X 100 for 3 min. The slides were mounted with 4′,6-diamidino-2-phenylindole (DAPI) for nucleus staining. The intracellular fluorescence of Coumarin-6 was examined using a fluorescence microscope. Coumarin-6 intracellular fluorescence was observed in the fluorescein isothiocyanate (FITC) filter, which shows fluorescence emission in the range of 510-560 nm [8].

### 3.2.6.7. Quantitative real-time polymerase chain reaction (PCR) analysis for expression of TNF-α in psoriasis induced model

The in-vitro psoriasis model was developed in HaCat cells using imiquimod (IMQ). HaCaT cells (2 x $10^6$ cells/mL) were cultured in 6 well plate in DMEM media with 10% FBS. The cells were treated with 5mM of $CaCl_2$ initially, and after 4 h, cells were treated with 100 μM IMQ and incubated for 24 h at 37 ºC. The differentiated cells were treated with the $IC_{50}$ dose of Apremilast and SLNs. The study was performed in four groups, untreated HaCaT cells (negative control), psoriasis induced HaCaT cells (positive control), and psoriasis induced HaCaT cells treated with free drug and nanoformulation. After treatment, the cells were incubated for 72 h, and total RNA extraction was performed using TRI Reagent® solution (TRIzol). The final RNA concentration was analyzed using Nanodrop. Further, the adequate concentration of RNA was taken to synthesize 1 μg/mL of cDNA using the RevertAid cDNA synthesis kit. All the qPCR studies were performed on CFX Thermocycler (Biorad). The transcript levels of the genes of interest were measured by quantitative RT-PCR (qRT-PCR). The qRT-PCR reactions were performed using the SYBR Green qRT-PCR. The data were normalized to the level of glyceraldehyde 3-phosphate dehydrogenase (GAPDH) housekeeping gene. The primers used for qPCR were TNF-α and GAPDH (GADPH sequence Forward (5'-3') ACCCAGAAGACTGTGGATGG, Reverse (5'-3')-TCTAGACGGCAGGTCAGGTC, TNF-α Sequence Forward (5'-3')-GATGGCAGAGAGGAGGTTGAC, Reverse (5'-3')-GAAAGCATGATCCGGGACGTG). The $C_t$ values of positive control, free drug-treated, and SLNs dispersion treated IMQ-induced psoriasis HaCaT cells were determined and stated concerning fold change over the negative control [15,16].

### 3.2.7. Preparation of Apremilast loaded SLNs gel and free drug-loaded gel

Optimized SLNs dispersion were formulated into the gel using Carbopol 974P as a gelling agent. The Carbopol was passed through sieve #60 before adding to SLNs dispersion. Passing through a sieve prevents agglomeration and minimizes lump formation. Carbopol added SLNs dispersion was neutralized using 100 µL of triethanolamine to form the gel. The optimized gel formulation was evaluated for further characterization. The plain emulsion was prepared by dissolving 150 mg of drug in oleic acid at 60 °C, and polysorbate 80 was added to the batch quantity of water separately. The drug oil blend was transferred into the water phase and mixed thoroughly for emulsion formation. A 1% batch quantity of isopropyl alcohol was added to the water phase as it acts as a co-surfactant and permeation enhancer. The prepared free drug-loaded emulsion was loaded into the hydrogel, similar to nanocarriers preparation using Carbopol 974P [17].

### 3.2.8. Characterization of Apremilast loaded SLNs gel

#### 3.2.8.1. Rheological behavior

The Apremilast loaded SLNs gel was evaluated for rheological parameters viscosity, amplitude test, and frequency sweep test using Rheometer MCR 92 (Anton-Paar Pvt. Ltd.). The tests were performed using a cone spindle with a 0.05 mm sample gap at a constant shear rate of 50 $s^{-1}$. The amplitude test of gel preparation was evaluated at a shear strain ranging from 0.1-100% at constant angular frequency 10 $s^{-1}$. The frequency test was assessed at an angular frequency ranging from 0.1-100 rad/s to determine the viscoelastic properties (storage modulus G', loss modulus G", and complex viscosity) were also measured. The study was executed at 32 ± 1 °C temperature to mimic the skin surface area's temperature as the solid gel to liquid phase transition ensues [18,19].

### 3.2.8.2. Occlusive Test

Selected Apremilast loaded SLNs gel, and free drug-loaded gel were evaluated for occlusion properties by in-vitro occlusion test. Glass vials (a capacity of 15 mL) with a diameter of 2.1 cm (wide mouth) were filled with water and covered with cellulose acetate membrane (Whatman number 6, cutoff size of 3 mm, USA). The selected Apremilast-loaded SLNs gel and the free drug-loaded gel were applied thoroughly on the cellulose acetate membrane, and all vials are maintained at 37 ± 0.5 °C for 48 h. One set of vials were kept without the application of the sample onto the cellulose acetate membrane. The weight of water before and after 24 and 48 h were recorded. The occlusion factor was calculated using equation 3.3.

$$F = \frac{A-B}{A} \qquad \text{(Eq. 3.3)}$$

F in equation 3.3 indicates the occlusion factor, A is the water loss without the sample, and B is the water loss with Apremilast loaded gel formulation [20].

### 3.2.8.3. Ex-vivo skin permeation studies

The ex-vivo skin permeation study was performed on goat skin using Franz diffusion cells with a contact surface area of 1.13 $cm^2$. Initially, goat ears were collected from the slaughterhouse, and the dorsal portion of goat ear skin was shaved using an animal hair clipper. The skin was mounted between the donor and receptor compartment, with the epidermis facing towards the donor. The receptor compartment was filled with of phosphate buffer saline (pH 7.4) as release media. The prepared free drug-loaded gel and Apremilast-loaded SLNs gel were applied in the donor compartment and spread over the epidermis. The diffusion cell assembly was placed on a magnetic stirrer at 200 rpm, and complete assembly was maintained at 32 ± 1 °C. Aliquots of 1 mL were collected at pre-determined time intervals (0.5, 1, 2, 4, 6, 8, 10, 12, 18, and 24 h), and an equal volume of fresh medium was replaced to maintain sink conditions. The amount of drug permeated was estimated using a validated HPLC method. The steady-state

transdermal flux ($J_{ss}$, µg/h/cm$^2$) and permeability coefficient ($K_p$, cm/h) were calculated from the data of the ex-vivo study. The $J_{ss}$ and $K_p$ are calculated using equations 3.4 and 3.5. The slope of the ex-vivo diffusion study indicates dQ/dt, viz. steady-state flux ($J_{ss}$) and permeability coefficient were calculated using $J_{ss}$ and mass of the drug in the donor compartment ($C_o$) [21,22].

$$J_{ss} = \frac{dQ}{A.dt} \quad \text{(Eq. 3.4)}$$

$$K_p = \frac{J_{ss}}{C_o} \quad \text{(Eq. 3.5)}$$

### 3.2.8.4. Dermal retention studies

After completing ex-vivo skin permeation studies, the skin was washed thrice with phosphate buffer saline to remove the residual drug from the superficial layer. The stratum corneum was separated using a tape stripping technique (validated by the weighing method). The remaining viable skin was chopped into pieces, and the drug retained in the skin was extracted by sonicating for 2 h and followed by homogenization. The extracted solution was subjected to centrifugation to separate the tissue matrix and the supernatant solution. The supernatant drug solution was further filtered through a 0.22 µm filter and analyzed by a validated HPLC method [21].

### 3.2.8.5. Ex-vivo dermal distribution studies

The ex-vivo dermal distribution of designed SLNs was evaluated performed with Coumarin-6 loaded SLNs on goat ear skin using Franz diffusion cell. The skin was processed and mounted on a Franz diffusion cell, as mentioned in the above section (ex-vivo skin permeation study). The receptor compartment was filled with phosphate buffer saline (pH 7.4). The Coumarin-6 loaded SLNs formulation and free Coumarin-6 equivalent to 100 µg were added to the donor

compartment separately. The whole experimental setup was maintained at a temperature of 32 ± 1 °C at 200 RPM. The treatment was done at 8 h and 16 h, and then the skin samples were collected. The collected skin samples were washed thoroughly with the saline buffer to remove surface-bound Coumarin-6. The cleaned skin sample was mounted onto a freezing microtome to section into micron size, and the samples were observed under a fluorescent microscope. The bright-field image and fluorescent portion images were collected using a ZEISS optical microscope [23].

#### 3.2.8.6. Dermatokinetic estimation

The drug concentration in skin layers (epidermis, dermis) at different time intervals was determined by a dermatokinetic study. The stratum corneum is the rate-limiting layer, whereas there is a need to determine drug retention in different layers. The drug is prone to elimination or degradation by skin enzymes. The absorption through the skin is concentration-dependent, to increase the maximum concentration in the skin layers, a high concentration drug is applied in conventional delivery systems. These parameters affect the kinetics of the drug on topical application.

Dermatokinetic studies were performed on goat ear skin using Franz diffusion cell as mentioned in the above section (ex-vivo skin permeation study). The fresh skin collected from the slaughterhouse was used to mimic the in-vivo metabolic conditions, and the study was initiated within two hours (the skin was maintained in freeze condition). The study was performed for the Apremilast loaded SLNs gel and free drug-loaded gel at pre-determined time points. After completion of the study, the skin was rinsed with the saline buffer and separated into the epidermis and dermis. The separated layers were subjected to drug extraction using acetonitrile. The drug extracted was processed by a validated solid-phase extraction technique to minimize the effect of the tissue matrix. The collected samples were filtered using a 0.22

µm filter and analyzed using a validated HPLC method. The Apremilast concentration (µg/cm$^2$) estimated in the epidermis and dermis were plotted, and dermatokinetic parameters were evaluated. For estimation of $T_{max}$, $C_{max}$, $AUC_{0–24h,}$ and $K_e$, the non-compartmental pharmacokinetic model was employed [9,24].

### 3.2.9. In-vivo studies

#### 3.2.9.1. Animals

All experimental protocols were approved by the Institutional Animal Ethics Committee (IAEC) before the commencement of work (Protocol No. IAEC/RES/24/06/Rev-1/28/28). Swiss albino mice 8-10 weeks old with an average weight of 35.87 ± 1.55 g were used to determine skin retention and signs of irritation of selected formulation. All mice were placed in the polyacrylic cages and housed under a maintained 12 h/12 h light/dark cycle at ambient temperature (22 ± 3 ºC) with 65% relative humidity. The food and water were provided *adlibitum* throughout the study period.

#### 3.2.9.2. Skin retention and Skin irritation study

The animals were divided into two groups. The two groups of animals were applied with each Apremilast-loaded SLNs gel and free drug-loaded gel. The gel was applied to the dorsal surface of the skin (2 cm$^2$) in each group at a 75 mg/cm$^2$ dose (the strength of gel was 0.05% w/w). After 12 h and 24 h, one group treated with each formulation was euthanized, respectively. The skin tissue was collected and processed for skin retention and histology study [23,25]. The collected skin was processed for histology studies to determine any changes in skin morphology. The skin samples were fixed 10% formaldehyde solution and embedded in paraffin and subjected to sectioning and hematoxylin and eosin (H&E) staining. The skin retention studies were performed as mentioned in dermal retention studies. The skin was subjected to tape stripping (10 tape strips) to separate the stratum corneum, and further, the

viable part of the skin was subjected for extraction of the drug. The skin extraction was subject to centrifugation to separate the skin residuals. The collected supernatant samples were filtered using a 0.22 µm filter and analyzed using the HPLC method [26,27].

### 3.2.10. Storage stability of Apremilast loaded SLNs gel

The selected formulation was evaluated for its capability to hold its physical and chemical characteristics. The prepared Apremilast-loaded SLNs gel were evaluated for stability up to three months at 4 °C and 25 °C. The Apremilast loaded SLNs gel formulation was evaluated for particle size integrity (using Malvern Zetasizer as mentioned above section 3.2.6.2) and the assay using validated stability-indicating HPLC method [8].

### 3.2.11. Statistical analysis

The statistical analysis was performed for the data obtained from three individual experiments. GraphPad Prism 5.0 was utilized for statistical analysis. The mean of the two groups was compared using two-way ANOVA, and the value at $p < 0.05$ was considered to be statistically significant.

## 3.3. Results and Discussion

### 3.3.1. Screening of solid lipids and surfactants

Lipid selection for the development of the SLNs was performed by evaluating the solubility of Apremilast in different melted lipids. High solubility indicates enhanced entrapment efficiency and increased drug loading with reduced drug expulsion on storage. The solubility of Apremilast in different lipids is represented in **Table 3.1**. As Apremilast exhibited the highest solubility in Precirol ATO5 compared to other lipids and selected for the preparation of SLNs. For the selection of the surfactant, SLNs formulations were prepared using Precirol ATO5 as the lipid with different surfactants at a fixed concentration of 0.75% (w/w) with varied HLB

values maintaining all process and formulation parameters constant. The size and PDI of SLNs prepared with poloxamer F127, polysorbate 80, and Kolliphor CS 12 were found to be 149.6 ± 2.01 nm (0.248) 96.80 ± 2.58 nm (0.403), and 149.7 ± 7.26 nm (0.268), respectively. The entrapment efficiency of poloxamer F127, polysorbate 80, and Kolliphor CS 12 were 43.29 ± 0.42%, 50.65 ± 0.91%, and 64.88 ± 0.76%, respectively. Based on this observation, Kolliphor CS 12 was selected due to its contribution for the small particle size, low polydispersity index, and high entrapment efficiency for SLNs. Kolliphor CS 12 is a non-ionic surfactant widely used for o/w emulsion for topical application. It is highly suitable for the hot process and stable in a broad pH range (acidic, basic, and ionic excipients). The selected surfactant with the desired RHLB of lipids provided small particle size and uniform distribution by stabilizing the lipid-water interface.

### 3.3.2. Drug excipient compatibility study and solution stability study in release media

The result indicated there was no change in the physical appearance of the drug-excipient mixture. The change in the percent assay of the drug was found to be not significant (less than 1%). This indicated the absence of interaction between selected excipients and Apremilast. The solution stability study results depicted that there was no degradation of Apremilast (Assay > 99.00 %) in release media up to 48 h.

**Table 3.1.** Solubility of the drug in the lipid by physical observation technique (n=3).

| S.No. | Lipid | Quantity of lipid in mg required to solubilize 2 mg drug |
|---|---|---|
| 1 | Glyceryl mono stearate | 479.8 ± 2.66 |
| 2 | Stearic acid | 424.7 ± 2.17 |
| 3 | Precirol®ATO5 | 344.8 ± 3.05 |
| 4 | Comptriol 888 ATO | 430.7 ± 2.95 |
| 5 | Dynasan 114 | 443.8 ± 2.29 |

### 3.3.3. Identification of quality target product profile and critical quality attributes

The identification of the QTPP initiated the QbD approach for the preparation of SLNs. The selected QTPP for Apremilast SLNs is listed in **Table 3.2**. The CQAs were selected from the QTPP, which were found to affect the finished product characteristics. The particle size, entrapment efficiency, particle size distribution, zeta potential, drug release, and retention time were identified as CQAs of Apremilast loaded SLNs and can show a high impact on the quality of the product as justified in **Table 3.3.**

**Table 3.2.** The quality target product profile of Apremilast loaded SLNs

| **Quality target product profile (QTPP)** | | |
|---|---|---|
| **Target Product profile** | **Target** | **Justification** |
| Dosage form | SLNs dispersion loaded gel | To improve permeation and retention in the skin with the ease of topical application. |
| Route of administration | Topical | To minimize the systemic effects of oral therapy and enhance the localized action. |
| Dose strength | 0.05% w/w | The dose within the minimum effective concentration range |
| Appearance | White smooth textured gel | Smooth gel free from grittiness, odour, or colour. With elegance with acceptable patient compliance. |
| Particle size | < 200 nm | To improve the permeation through the stratum corneum |
| Entrapment Efficiency | Maximum | Higher entrapment helps in minimizing the lipid quantity (enhanced drug loading). |
| Release | Sustained release | It favors the prolonged release within skin layers and minimizes systemic absorption. |
| Occlusion | Maximum occlusion | Maximum occlusion favors a maximum reduction of TEWL and enhances the permeation. |

### 3.3.4. Risk identification and risk assessment

The risk identification was performed, and critical process parameters and critical material attributes were identified using the constructed Ishikawa diagram depicted in **Figure 3.1**. The

factors such as the amount of lipid, surfactant concentration, stirring speed, stirring time, temperature, and sonication time during the process were considered the potential risk as per Risk Estimation Matrix (REM), affecting the particle size PDI, entrapment, and drug release. The REM assessment of the material and process attributes is depicted in **Table 3.4**.

**Table 3.3.** Critical quality attributes for Apremilast loaded SLNs embedded gel

| **Critical Quality Attributes** | **Justification** |
|---|---|
| **Particle size** | The smaller the size, the greater the permeation through the stratum corneum. |
| **Particle size distribution** | The uniform particle size distribution favors uniform drug release, permeation and uniform drug loading (reduced vacillations). |
| **Entrapment efficiency** | Maximum entrapment facilitates increasing drug loading ability. |
| **Percent drug release** | For prolonged action within skin layers can be attained by sustained release. |
| **Retention in skin layers** | Reduce unwanted systemic effects by the reduction in systemic absorption. |

**Table 3.4.** Risk Estimation Matrix (REM) for initial risk assessment of different material attributes and process parameters by qualitative analysis.

| **Critical quality attributes** | **Critical material attributes and Critical process parameters** | | | | | |
|---|---|---|---|---|---|---|
| | **Amount of Lipid** | **Surfactant concentration** | **Sonication Time** | **Stirring speed** | **Stirring Time** | **Temperature of surfactant solution** |
| **Particle size** | High | High | High | Medium | Low | High |
| **Polydispersibility Index (PDI)** | High | High | High | High | Low | Low |
| **Entrapment efficiency** | High | Medium | Medium | Low | High | Low |
| **% Drug release** | High | High | Low | Low | Medium | Medium |

The FMEA analysis provided the rank order scoring based on various factors from initial trials and reported studies. The effect of material attributes and process parameters was evaluated to

estimate the risk potential of the SLNs dispersion. The rank order value was set on a scale of 5 and RPN scores above 30 was considered as critical attributes. **Table 3.5** depicts the FMEA rank-order score based on the effects of material attributes and process parameters. The CMAs and CPPs affecting the quality of the finished product were predicted using FMEA analysis. The RPN scores were found to be more than 30 for amount of lipid and the surfactant concentration and considered as the CMAs affecting the entrapment efficiency and size of the Apremilast loaded SLNs. Similarly, the sonication time was selected as CPPs affecting size of the size and entrapment efficiency of the Apremilast-loaded SLNs.

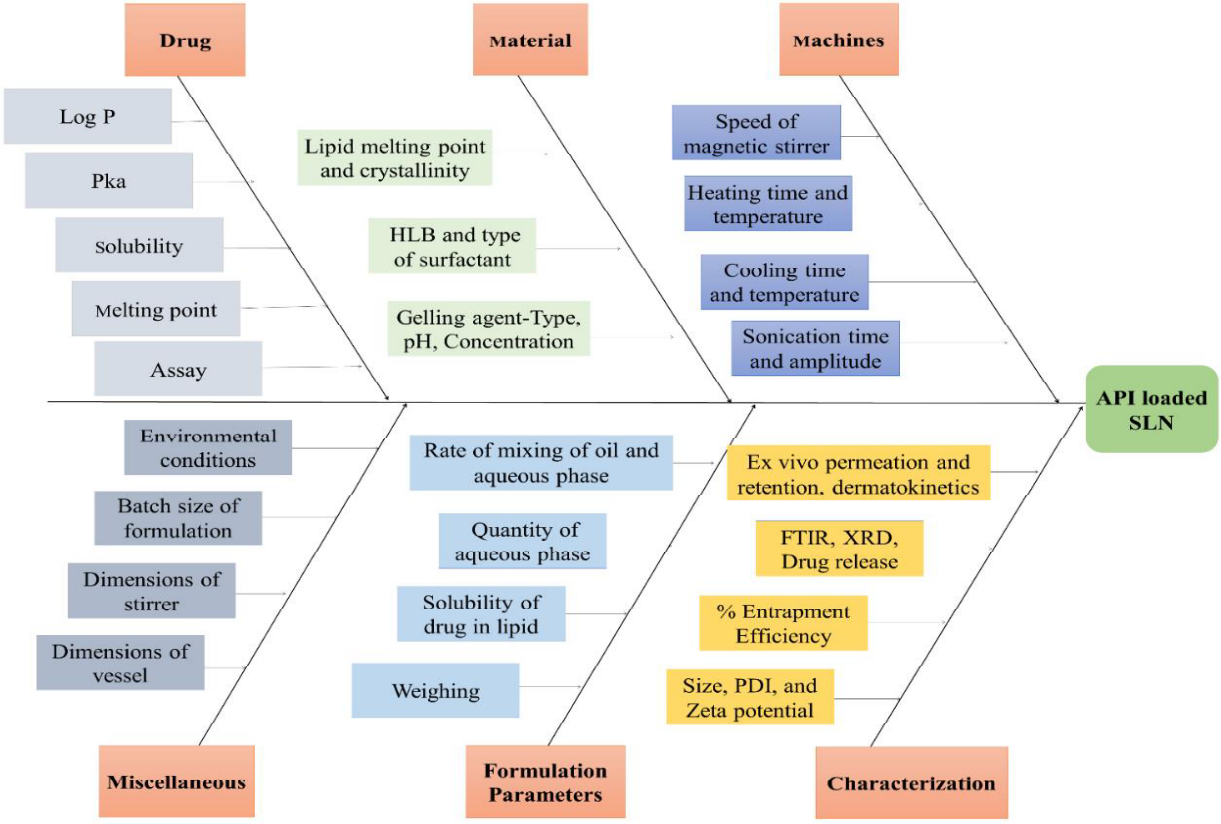


**Figure 3.1.** Ishikawa diagram depicting the potential CMAs and CPPs that affect the CQAs of Apremilast loaded SLNs formulation.

**Table 3.5.** Failure Mode Evaluation and Analysis (FMEA) rank-order score based on the effects of material attributes and process parameters.

| Material attributes & Process parameters | Severity (S) | Detectability (D) | Occurrence (O) | RPN score |
|---|---|---|---|---|
| **Amount of Lipid** | 4 | 3 | 4 | 48 |
| **Surfactant concentration** | 4 | 3 | 4 | 48 |
| **Sonication Time** | 4 | 3 | 4 | 48 |
| **Stirring speed** | 3 | 3 | 2 | 18 |
| **Stirring Time** | 2 | 3 | 2 | 12 |
| **Temperature of surfactant solution** | 4 | 2 | 2 | 16 |

### 3.3.5. Optimization by the design of experiments

The formulations were optimized for selected material attributes and process parameters i.e. amount of lipid, surfactant concentration, and sonication time. The particle size and drug entrapment were selected as critical quality attributes. Box-Behnken experimental design with 17 trials was employed with 3 factors at 3 levels using Design-Expert software (Design-Expert® 8.0, State-Ease Inc., Minneapolis, USA) for formulation optimization. In this design, the amount of lipid, surfactant concentration, and sonication time (Independent variables) was studied at low, medium, and high-level concentrations. In concurrence to design, 17 batches were executed that are summarized in **Table 3.6**. Formulations were prepared by varying independent variables keeping all other parameters (process and formulation parameters) constant and investigated for particle size and entrapment efficiency as dependent (response) variables. The preservatives methylparaben and propylparaben were used in the concentrations of 0.2% w/v and 0.02% w/v, respectively and were kept constant in all trials. The use of propylparaben and methylparaben (1:10) in combination provides a synergistic effect as preservatives. The model efficiency and significance of the selected input factors were evaluated using analysis of variance.

**Table 3.6.** Experiment trials executed using Box-Behnken design and the obtained results (n=3).

| S.No. | Lipid (mg) | % Surfactant | Sonication time (min) | Size (nm) | % Entrapment | PDI |
|---|---|---|---|---|---|---|
| 1 | 100 | 0.55 | 3.50 | 184.35 ±10.91 | 54.77 ± 1.56 | 0.279 |
| 2 | 100 | 0.55 | 3.50 | 165.55 ±12.47 | 57.25 ± 0.58 | 0.319 |
| 3 | 50 | 0.55 | 2.00 | 213.10 ±15.37 | 10.11 ± 1.92 | 0.700 |
| 4 | 50 | 0.55 | 5.00 | 69.85 ± 12.37 | 8.21 ± 8.17 | 0.414 |
| 5 | 150 | 0.55 | 2.00 | 195.95 ± 8.49 | 63.55 ± 4.34 | 0.315 |
| 6 | 100 | 0.10 | 5.00 | 221.50 ± 16.27 | 49.65 ± 2.21 | 0.397 |
| 7 | 100 | 0.55 | 3.50 | 123.40 ± 8.57 | 54.89 ± 2.49 | 0.290 |
| 8 | 150 | 1.00 | 3.50 | 110.80 ± 5.71 | 72.54 ± 3.39 | 0.310 |
| 9 | 50 | 1.00 | 3.50 | 88.70 ± 13.58 | 15.93 ± 3.75 | 0.440 |
| 10 | 100 | 0.10 | 2.00 | 278.15 ± 7.57 | 52.16 ± 3.25 | 0.375 |
| 11 | 100 | 0.55 | 3.50 | 190.95 ± 2.62 | 25.90 ± 4.53 | 0.254 |
| 12 | 100 | 1.00 | 2.00 | 123.85 ± 10.64 | 14.25 ± 2.05 | 0.558 |
| 13 | 100 | 1.00 | 5.00 | 83.05 ± 13.06 | 54.30 ± 6.01 | 0.290 |
| 14 | 150 | 0.55 | 5.00 | 140.55 ± 10.78 | 62.10 ± 5.58 | 0.248 |
| 15 | 100 | 0.55 | 3.50 | 124.10 ± 11.13 | 60.35 ± 1.66 | 0.268 |
| 16 | 50 | 0.10 | 3.50 | 152.05 ± 13.61 | 42.03 ± 3.89 | 0.341 |
| 17 | 150 | 0.10 | 3.50 | 404.00 ± 15.66 | 42.70 ± 4.30 | 0.993 |

* PDI was not considered as the response variable. Level for lipid amount: Low, Medium, High were 50 mg, 100 mg, and 150 mg respectively. Level for surfactant concentration: Low, Medium, High were 0.10%; 0.55%; and 1.00% respectively. Level for sonication time: Low, Medium, High were 2.00 min; 5.00 min; and 5.00 min respectively.

### 3.3.5.1. Effect of independent variables on particle size

The average particle size of Apremilast loaded SLNs were in the range of 69.85 to 404.00 nm as represented in **Table 3.6**. The model (Quadratic model) was found to be significant with a 6.17 F-value. The ANOVA for the responses are depicted in **Table 3.7**. The contour plot and 3D plot of the response variable particle size are depicted in **Figure 3.2 A** and **Figure 3.2 B**.

The Lack of Fit was found to be insignificant with F-value of 2.51 compared to the pure error. The coded values of selected independent variables are depicted in the regression equation 3.6.

$$\textbf{Size} = 252.1353 + 0.821022A - 89.4488B - 33.7643C - 2.55389AB + 0.292833AC + 5.87037BC + 0.001889A^2 + 130.8457B^2 - 3.34611C^2 \quad \text{(Eq. 3.6)}$$

The positive symbol in regression equation represents the collusive effect indicating an increase in response value with the respective input variable. The regression equation's negative symbol represents the decrease in response value with the respective input variable. The lack of fit indicates the dissimilarity in the best fit model's data and affords the competence of the model fitting of experimental results. The insignificant lack of fit in experimental results indicated the best fit for the model. The regression equation 3.6 expresses an increase in particle size with an increase in amount of lipid. With the increase in lipid amount, the viscosity of the dispersed phase (melted lipid phase) will increase which may results in increased particle size of the dispersion. The reduction in particle size was observed with an increase in the % surfactant concentration and sonication time. The surfactant may reduce the surface tension at the lipid-water interface and enhance the particle's stabilization which results in reduced particle size. The increase in sonication reduces the size of the SLNs due to breaking the larger particles into small particles. The S/N ratio of the model is measured by adequate precision. A ratio above 4 is more desirable and indicates the adequacy of the model. The S/N ratio of size was found to be 9.853 that showed the adequacy of the obtained model.

### 3.3.5.2. Effect of independent variables on entrapment efficiency

The average entrapment efficiency of Apremilast loaded SLNs were in the range of 8.22 to 72.55 nm, as represented in **Table 3.6.** The Quadratic model with a 2.82 F-value indicates the significance of the model. The contour plot and 3D graph of the response variable entrapment efficiency are depicted in **Figure 3.2 C** and **Figure 3.2 D**. The Lack of Fit was insignificant,

with F-value of 1.18 compared to the pure error. The coded values of selected independent variables are represented in the regression equation 3.7.

$$\textbf{Entrapment efficiency} = -1.04771 + 0.620644A - 123.464B + 17.87526C + 0.621562AB + 0.001646AC + 15.75856BC - 0.00278A^2 - 1.85806B^2 - 3.40761C^2 \quad \text{(Eq. 3.7)}$$

The regression equation 3.7 expresses the increase in the entrapment with an increase in amount of lipid. It was expected due to the partitioning of Apremilast into the lipid phase. The reduced entrapment efficiency was observed with an increase in the % surfactant concentration. The surfactant may enhance the drug's solubility and increase the free drug (dissolved) which may result in reduced entrapment efficiency.

**Table 3.7.** ANOVA for response particle Size and entrapment efficiency.

| **Response** | **Particle Size** | | **Entrapment efficiency** | |
|---|---|---|---|---|
| Source | F-value | p-value | F-value | p-value |
| Model (significant) | 6.16636 | 0.0128 | 2.820437 | 0.0927 |
| A- Amount of lipid | 7.793482 | 0.0268 | 16.04512 | 0.0052 |
| B-Surfactant concentration | 30.61502 | 0.0009 | 0.515215 | 0.4961 |
| C-Sonication time | 6.36679 | 0.0396 | 0.693997 | 0.4323 |
| AB | 7.672957 | 0.0277 | 3.703618 | 0.0957 |
| AC | 1.120875 | 0.3249 | 0.000289 | 0.9869 |
| BC | 0.036487 | 0.8539 | 2.142556 | 0.1867 |
| $A^2$ | 0.054524 | 0.8221 | 0.964893 | 0.3587 |
| $B^2$ | 1.717271 | 0.2314 | 0.002822 | 0.9591 |
| $C^2$ | 0.138649 | 0.7206 | 1.171744 | 0.3149 |

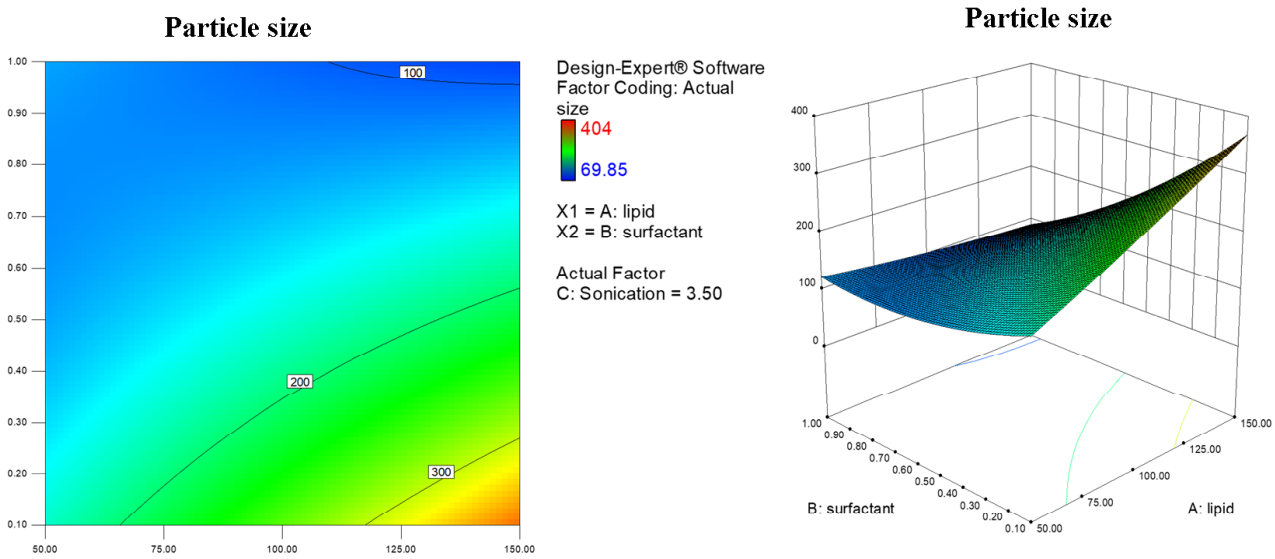


**Figure 3.2 A.** Box-Behnken optimization contour plot graph depicting effect of independent variables on particle size. **Figure 3.2 B**. Box-Behnken optimization 3D graph depicting effect of independent variables on particle size.

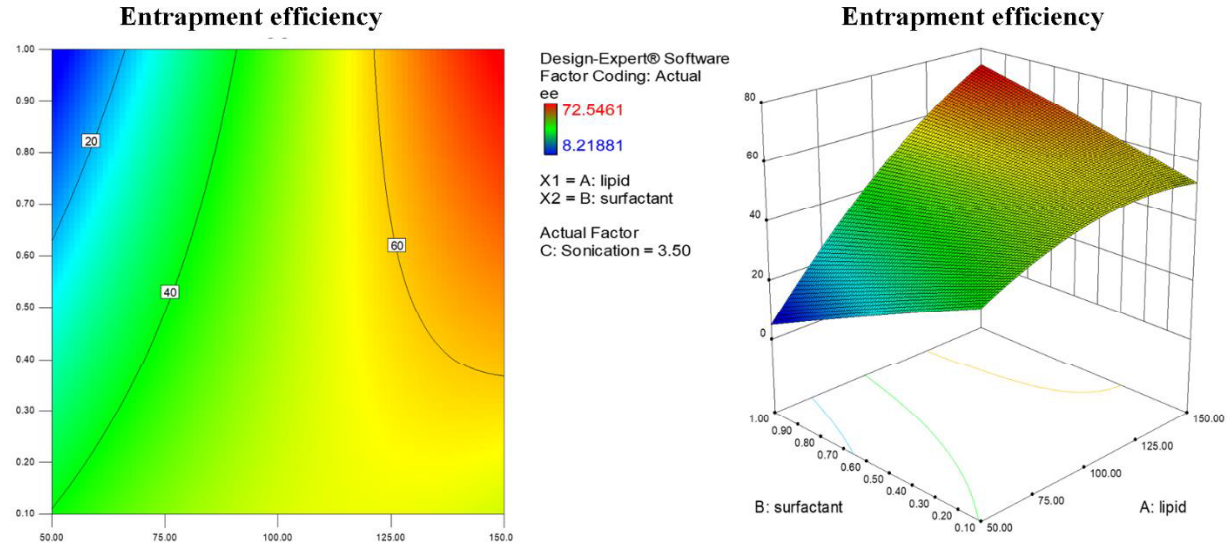


**Figure 3.2 C.** Box-Behnken optimization contour plot graph depicting the effect of independent variables on entrapment efficiency. **Figure 3.2 D.** Box-Behnken optimization 3D graph depicting the effect of independent variables on entrapment efficiency.

The increase in sonication enhanced the entrapment. It was expected due to the conversion of maximum lipid to nano size as the microparticulate particles are separated from the formulation, which reduced the entrapment efficiency in reduced sonication time. The S/N ratio

of entrapment efficiency was found to be 6.202 that showed the adequacy of the obtained model.

### 3.3.6. Validation of the design to select optimized batch

The Apremilast loaded SLNs formulation was optimized by the numerical and desirability method. The aim was to select the formulation with the highest entrapment efficiency and the smallest particle size. The summary of constraint criteria is depicted in **Table 3.8,** which is required to achieve the desired response. The Design-Expert software exemplified 43 solutions and higher desirability near to 1 was selected for preparing SLNs formulation. The design was validated using two formulations with amount of lipid (100 mg, 150 mg), surfactant concentration (0.55%) and sonication time (3.5 min, 5 min).

**Table 3.8.** Constraint criteria for achievement of desired response variable and deviation (%) calculation of SLNs formulation.

| **Parameter** | **Goal** | **Lower Limit** | **Upper Limit** |
|---|---|---|---|
| Amount of lipid (mg) | In range | 50 | 150 |
| Surfactant concentration (%) | In range | 0.1 | 1 |
| Sonication time (min) | In range | 2 | 5 |
| Particle size (nm) | Minimize | 69.85 | 404.00 |
| EE (%) | Maximize | 8.22 | 72.55 |

| **Deviation (%) calculation of Apremilast - SLNs formulation.** | | | | | | |
|---|---|---|---|---|---|---|
| **Parameter** | **Predicted values** | | **Actual values** | | **Deviation (%)** | |
| | **I batch** | **II batch** | **I batch** | **II batch** | **I batch** | **II batch** |
| Particle size (nm) | 157.67 | 180.76 | 127.95 | 164.13 | 29.72 | 16.63 |
| % EE | 50.64 | 60.99 | 60.60 | 63.97 | 9.97 | 2.98 |

The desirability graphs of particle size and entrapment efficiency of two validated batches are depicted in **Figure 3.3 (A-D).** The mean particle size of the formulation with 100 mg lipid was found to be 127.95 ± 3.95 nm, with 0.214 ± 0.019 PDI. The zeta potential and entrapment

efficiency of the optimized formulation were found to be -26.25 ± 1.41 mV and 60.6 ± 0.40%. The size of the formulation with 150 mg lipid was obtained as 164.13 ± 2.19 nm with 0.234 ± 0.031 PDI. The zeta potential and entrapment efficiency were found to be -21.37 ± 1.40 mV and 63.97 ± 0.102% with formulation of 150 mg lipid. The percent drug release of formulation with 100 mg lipid was more than 90% in the first 8 h. The percentage drug release of formulation with 150 mg lipid more than 90% was achieved after 12 h. The sustained release of the drug was achieved with 150 mg lipid. This was expected due to the solubility of the drug in the lipid component has retarded release. The formulation with 150 mg lipid (composition similar to batch no. 14) was selected for further characterization. The % deviation of the selected formulation with entrapment efficiency was 2.98%, and particle size was less than 16.63 nm showed the closeness of the predicted value to the actual value and confirming the design's desirability.

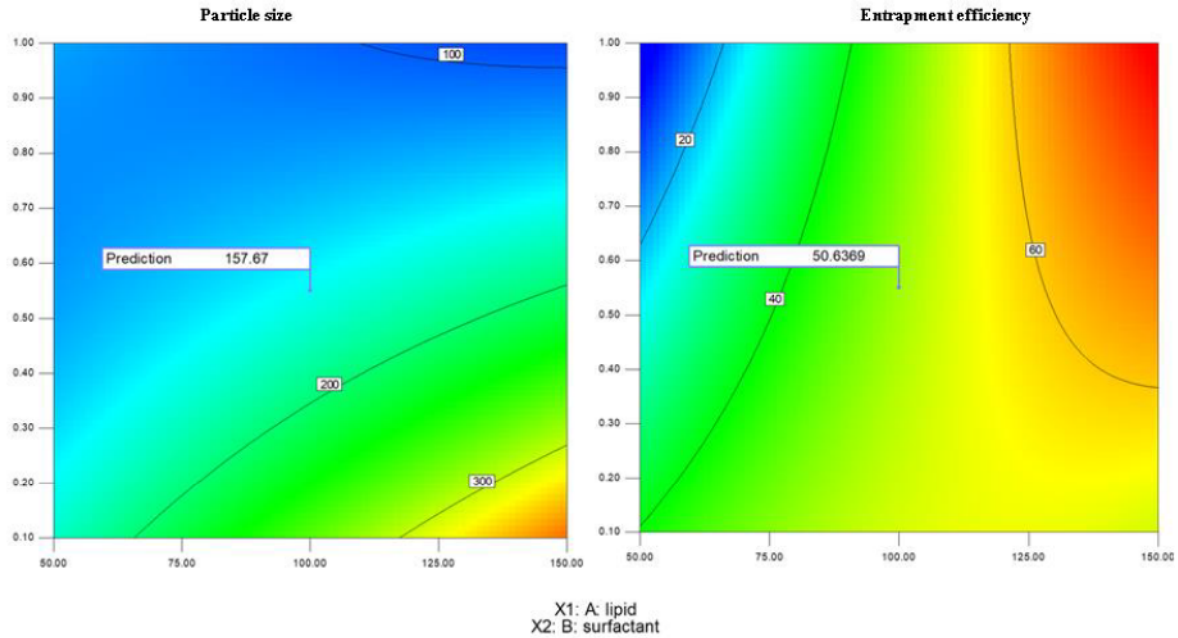


**Figure 3.3 A.** The desirability contour plot for particle size of the batch with 100 mg lipid. **Figure 3.3 B.** The desirability contour plot for entrapment efficiency of the batch with 100 mg lipid.

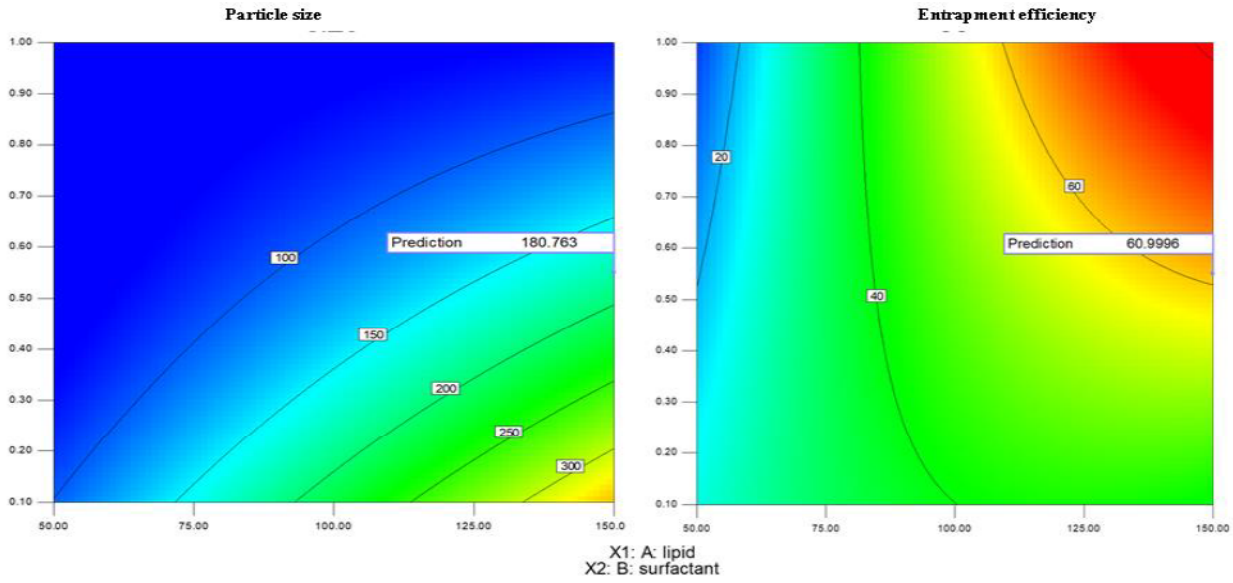


**Figure 3.3 C.** The desirability contour plot for particle size of the batch with 150 mg lipid. **Figure 3.3 D.** The desirability contour plot for entrapment efficiency of the batch with 150 mg lipid.

### 3.3.7. Scale-up Studies of the optimized batch

The study was scaled up to a maximum of 100 mL. The batch sizes with 10 mL, 50 mL and 100 mL were prepared using the parameters obtained in the design space. The composition was similar to batch no. 14, as mentioned in **Table 3.6**. The composition (formulation parameters) was kept constant, whereas sonication time was altered as it was a critical criterion in size reduction. The instrument efficiency directly impacts the size reduction, as the formulation parameters amount of lipid and surfactant concentration were increased proportionally to batch size. The vessel diameters had a critical role in the size reduction on sonication. The increase in the diameters (proportionally) and capacity of the probe sonicator had the minimum effect, whereas the larger diameter vessel altered the formulation parameters to a large extent. The sonication time for 10 mL and 50 mL was 3.5 min, and the sonication time for the 100 mL batch was 4.0 min. The particle size of the three formulations with 10 mL, 50 mL and 100 mL batch size were 148.33 nm ± 1.880 (0.252 PDI), 128.90 nm ± 0.556 (0.194 PDI) and 167.70

nm ± 1.500 (0.238 PDI), respectively. Entrapment efficiency was found to be 62.84 ± 1.07%, 60.20 ± 1.92%, 63.84 ± 0.93% for 10 mL, 50 mL and 100 mL batches, respectively.

### 3.3.8. Characterization of lipid nanocarriers

#### 3.3.8.1. Attenuated total reflection-Fourier transform infrared spectroscopy (ATR-FTIR)

The FTIR spectra were generated to study the interaction between Apremilast and formulation excipients. The Apremilast, physical mixture, and Apremilast loaded SLNs are presented in Supplementary **Figure 3.4 (A-C).** The spectra revealed that the absence of physicochemical interactions between the drug and other formulation excipients. The Apremilast characteristic peaks include the range of 3100 and 3500 $cm^{-1}$ indicating the amide group of Apremilast.

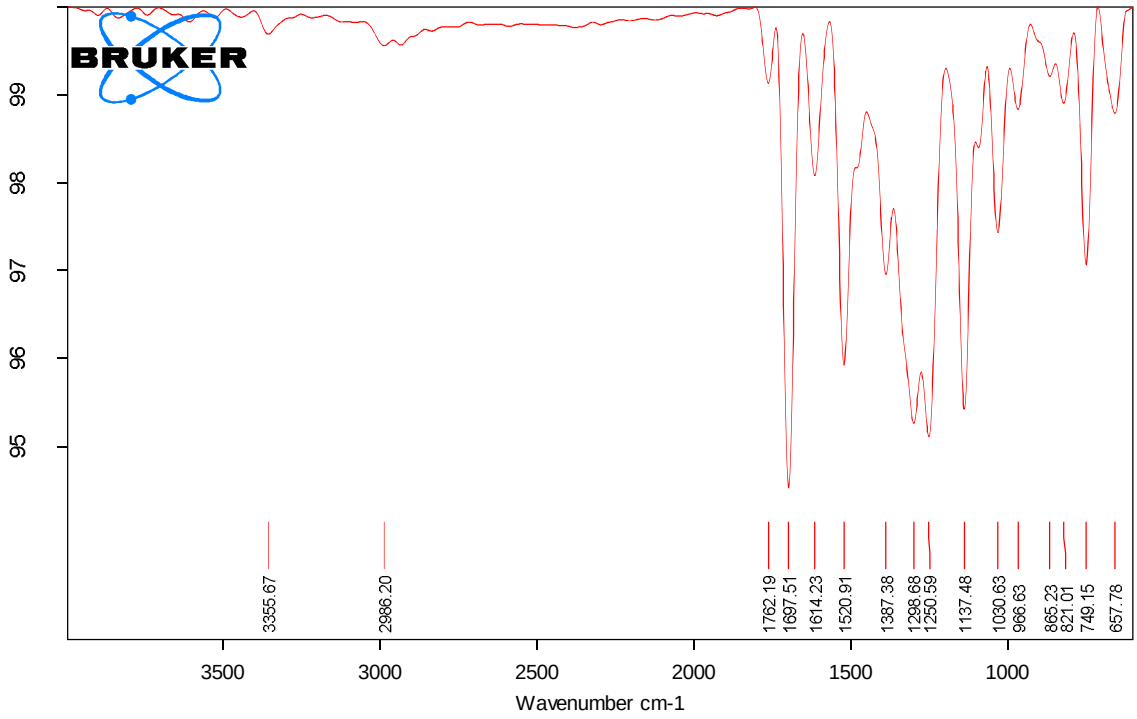


**Figure 3.4 A.** ATR spectra of Apremilast pure drug.

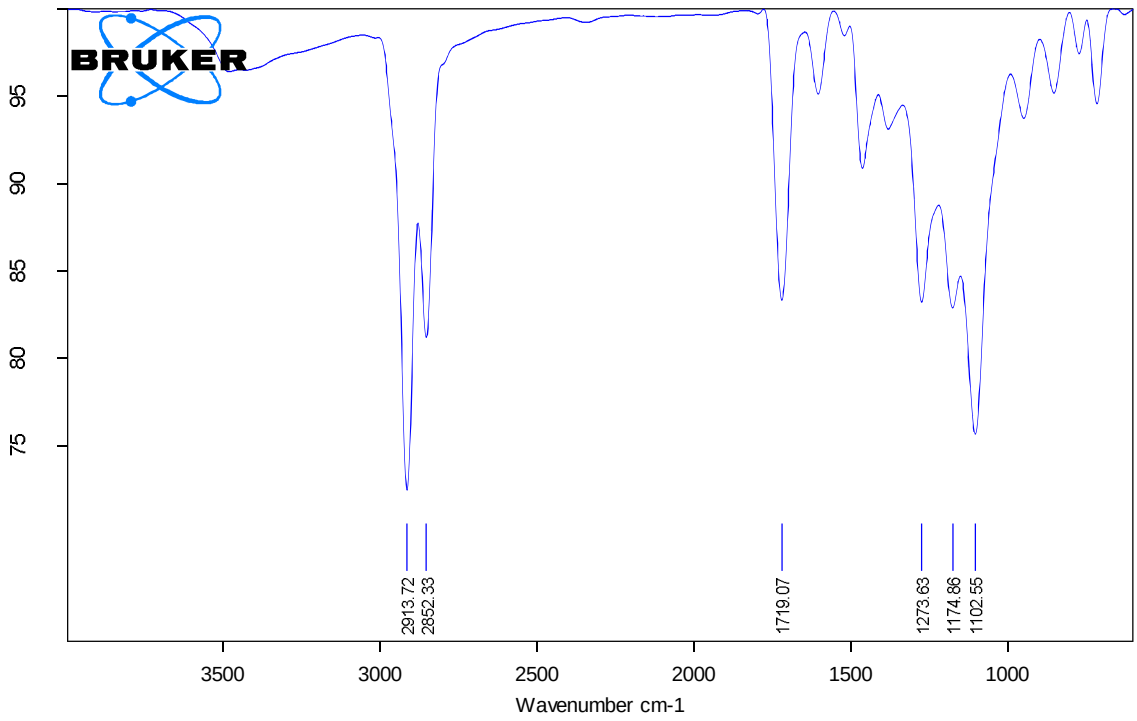


**Figure 3.4 B.** ATR spectra of Apremilast loaded SLNs.

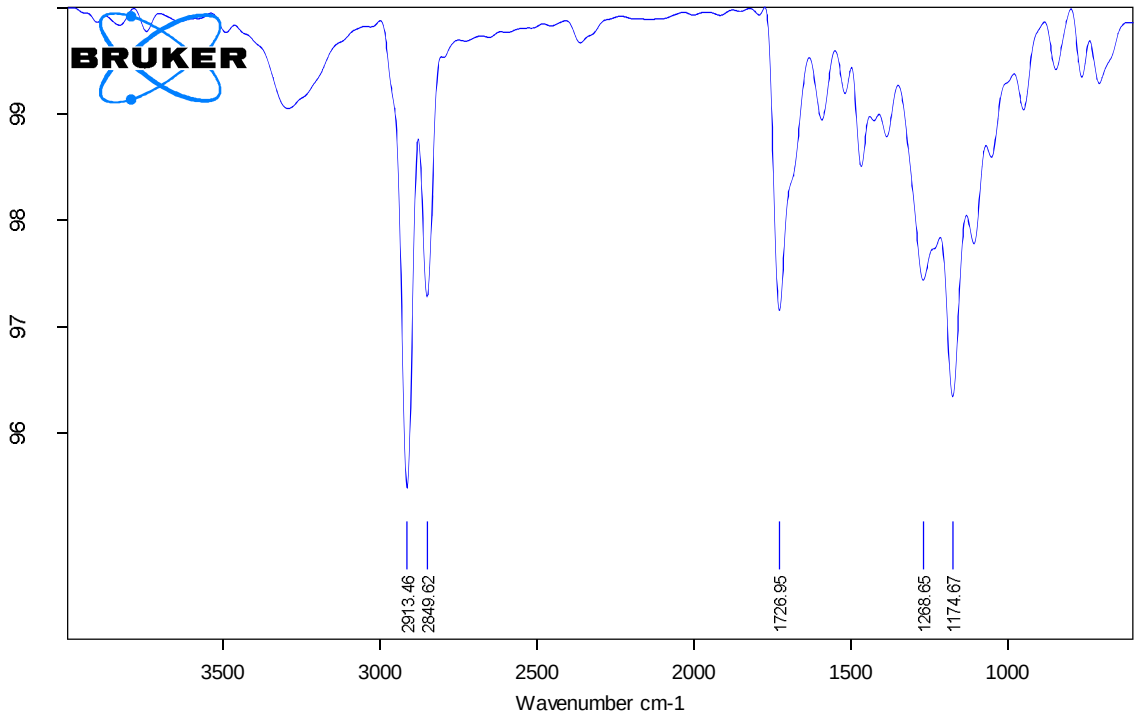


**Figure 3.4 C.** ATR spectra of Apremilast loaded SLNs excipients physical mixture.

The C=C (alkene) and C-C (alkane) peaks range from 1600 $cm^{-1}$ and 1300 $cm^{-1}$. The peaks in the range of 1100 $cm^{-1}$ and 1000 $cm^{-1}$ indicate the C-OH and C-O (ester bond), respectively. The study demonstrated no chemical interaction and good compatibility of the excipients with Apremilast in the SLNs formulation.

### 3.3.8.2. Particle size, Polydispersibility index (PDI), zeta potential measurement and entrapment efficiency

The particle size of the selected formulation was 167.70 nm ± 1.500 (0.238 PDI), respectively (depicted in **Figure 3.5**). The reported studies suggest that the lipid nanocarriers particle size less than 200 nm exhibit improved permeation [28]. The PDI less than 0.300 suggests the uniformity of the SLNs dispersion. The optimized formulation exhibited zeta potential of -23.5 ± 0.53 mV (depicted in **Figure 3.6)**. The zeta potential above ± 10 indicates stable electrostatic repulsion of the prepared dispersion which minimizes the particle's coalescence/aggregation. Entrapment efficiency was found to be 63.84 ± 0.93%. The results indicated that all batches exhibited similar characteristics. The SLNs morphology was spherical and in the range of 100 nm to 140 nm, as depicted in **Figure 3.7.**

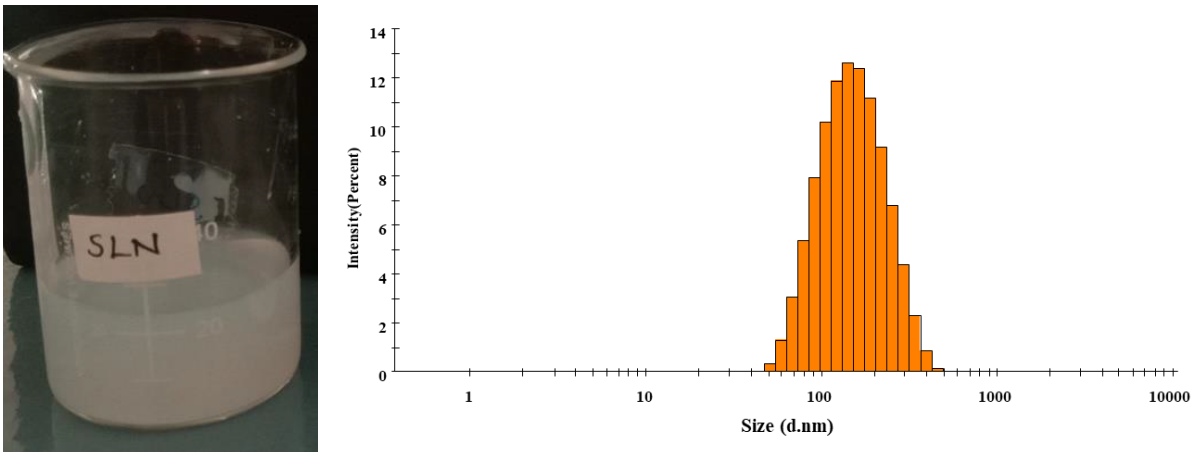


**Figure 3.5.** Apremilast loaded SLNs dispersion and particle size statistics graph.

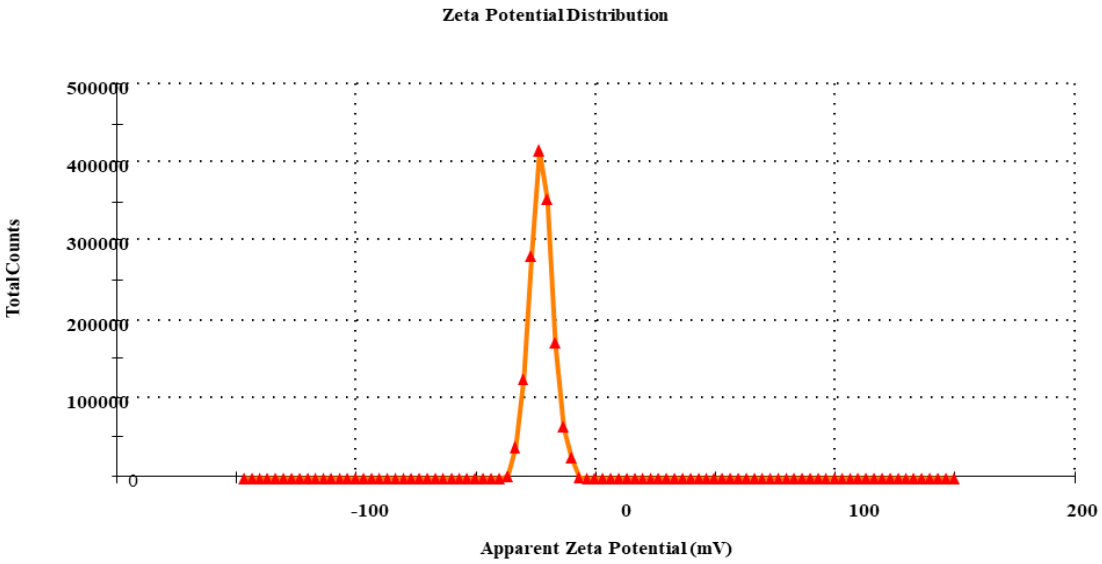


**Figure 3.6.** Apremilast loaded SLNs dispersion zeta potential graph.

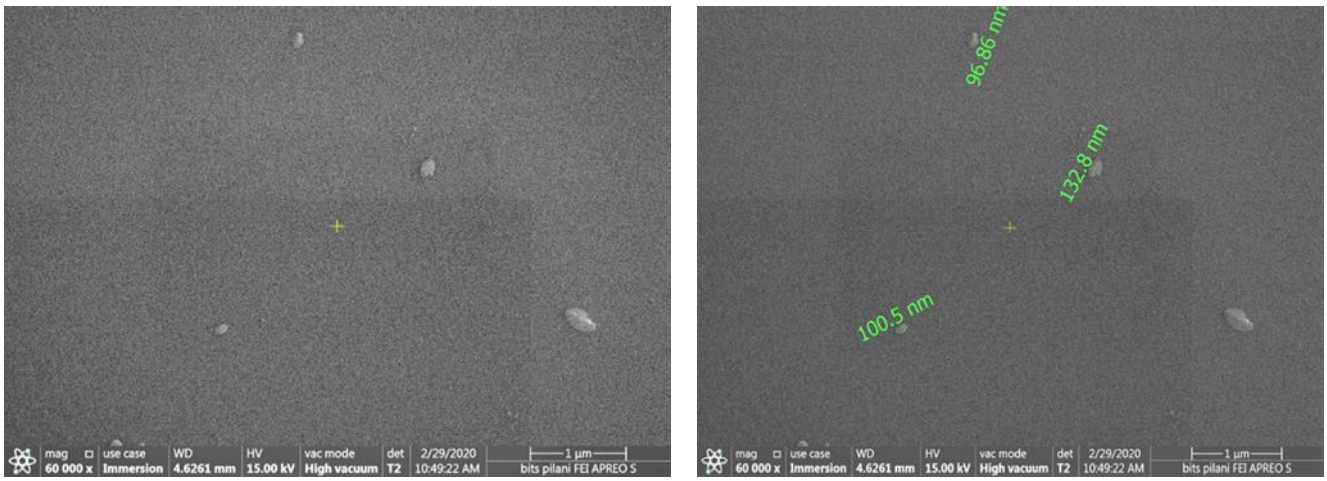


**Figure 3.7.** FESEM image of Apremilast loaded SLNs dispersion performed using Field Emission Scanning Electron Microscopy (Apreo Switch XT microscope).

### 3.3.8.3. In-vitro drug release studies

In-vitro release studies were performed for Apremilast loaded SLNs dispersion for all the three formulations (10 mL, 50 mL, and 100 mL batch size) and free drug solution. The % cumulative drug release study was performed for 24 h. The study was conducted in triplicate, and drug release curves are represented in **Figure 3.8**. The free drug solution showed a 100% drug release within the first 6 h. SLNs dispersion showed drug release up to 18 h with initial quick

release followed by slow release compared to free drug solution. The release kinetics evaluated using "DDSolver" complied in Table 3.9. The release of the SLNs dispersion, found to follow Korsmeyer-Peppas model as the best fit with the highest $r^2$ value and minimum Akaike information criterion (AIC). The n value obtained was less than 0.45 indicating the Fickian type diffusion. The n corresponds to the release exponent implying the mechanism of drug release. The drug release mechanism is followed by Fickian diffusion if n = 0.5 or n < 0.5. The release mechanism is considered as non-Fickian or anomalous diffusion mechanism, if 0.5 < n < 1.0. If n = 1.0, the mechanism is known as non-Fickian case II diffusion. It is reflected as the non-Fickian super-case II diffusion mechanism if n > 1.0, is followed [10]. The initial quick release was expected from the drug dispersed on the SLNs surface, and the drug dissolved in the lipid matrix released in a controlled manner. The impede in drug release from lipidic nanocarriers provides a slow release of the drugs in the skin layers and affords prolonged action.

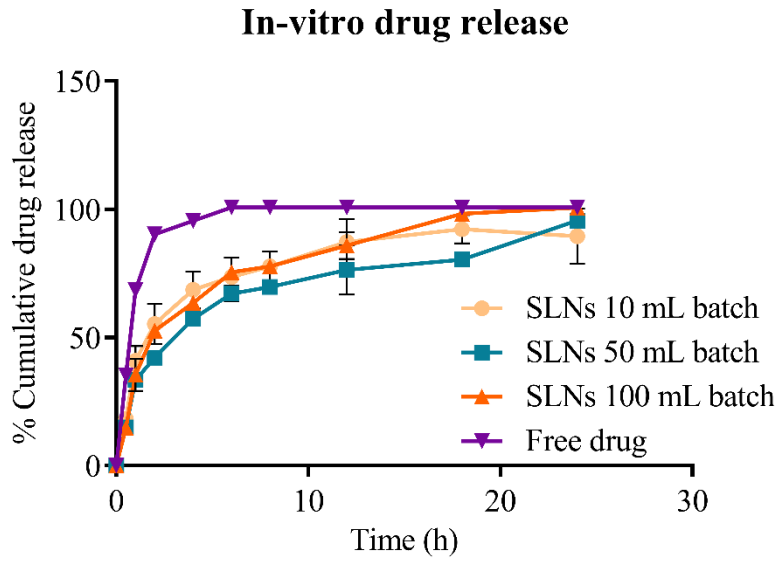


**Figure 3.8.** The in-vitro drug release profile of Apremilast loaded SLNs dispersion (10 mL, 50 mL and 100mL batch size) and free drug.

**Table 3.9.** Release kinetic mechanism data of Apremilast loaded SLNs dispersion

| Batch Size | | Zero-order | First-order | Higuchi | Korsmeyer-Peppas | Hixson-Crowell |
|---|---|---|---|---|---|---|
| **10 mL** | $R^2$ | 0.195 | 0.902 | 0.734 | 0.934 (n:0.272) | 0.782 |
| **10 mL** | AIC | 94.817 | 69.722 | 79.780 | 66.612 | 77.799 |
| **50 mL** | $R^2$ | 0.211 | 0.8872 | 0.883 | 0.965 (n:0.334) | 0.820 |
| **50 mL** | AIC | 89.951 | 70.511 | 70.879 | 59.404 | 75.135 |
| **100 mL** | $R^2$ | 0.176 | 0.952 | 0.870 | 0.958 (n:0.330) | 0.892 |
| **100 mL** | AIC | 92.797 | 64.324 | 74.332 | 63.669 | 72.414 |

### 3.3.8.4. Cytotoxicity study

The cytotoxicity study of Apremilast and Apremilast loaded SLNs was performed on HaCaT cell lines (immortalized human keratinocyte). These cells were preferred as 95% of epidermal skin cells are keratinocytes. The cytotoxicity results of Apremilast solution and Apremilast loaded SLNs dispersion on HaCaT cell lines were represented in **Figure 3.9.** Apremilast was relatively non-toxic against the keratinocyte cells. More than 50% of cell viability was noted with 20 nm concentration with Apremilast-loaded SLNs and free Apremilast solution. The results demonstrated that formulation excipients do not produce toxicity towards the keratinocytes cells ($p<0.05$) [29].

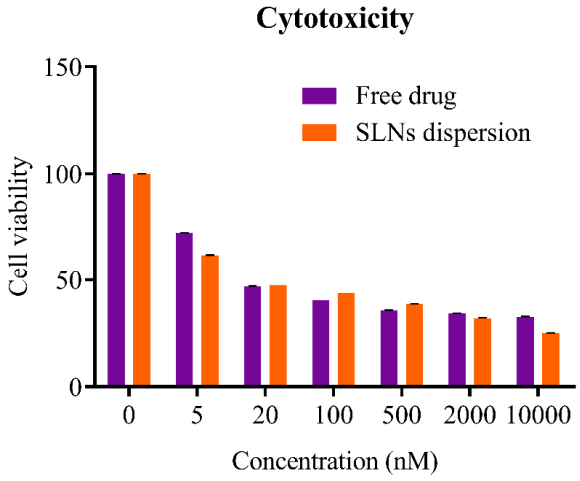


**Figure 3.9.** Graphical representation of cell viability of Apremilast loaded SLNs dispersion and free drug ($p<0.05$).

### 3.3.8.5. Cell uptake

The cell uptake study was performed by checking the Coumarin-6 (fluorescent dye) loaded SLNs at 1 h and 3 h intervals. The HaCaT cells treated with Coumarin-6 dispersion, and Coumarin-6 loaded SLNs. At 1 h interval, the Coumarin-6/DAPI ratio of Coumarin-6 loaded SLNs was 2.82 fold higher than Coumarin-6 dispersion. At 3 h interval, Coumarin loaded SLNs was found to be 2.17 fold higher than the Coumarin-6 dispersion. The fluorescence microscope images of cell uptake data and cell uptake intensity are represented in **Figures 3.10 A and 3.10 B**. The enhanced uptake was supposed due to the interaction between the cell membrane, the fatty acid chain of the lipid, and the nano size of the SLNs [30].

### 3.3.8.6. Expression of TNF-α in psoriasis induced model

IMQ, is a ligand for Toll-like receptors (TLR) 7 and TLR8 and a potent immune activator, is used for topical treatment of genital and perianal warts [31]. IMQ induced aggravation of psoriasis arises at both the treated area and, interestingly, also at separate skin sites which are unaffected previously. The efficacy of Apremilast free drug and SLNs dispersion in reducing TNF-α was studied on IMQ-induced psoriasis. The RNA isolated and gene expression quantification was performed and normalized to GAPDH. The results demonstrated a perceptible change in $C_t$ values in cells treated with free Apremilast and SLNs dispersion. There was a 3 fold more significant $C_t$ value reduction with SLNs dispersion and 1.6 fold with the free drug than the positive control (***$p<0.0001$; one-way ANOVA was performed). The results are presented in **Figure 3.11** [15,16]. The results showed the inhibition of the relative mRNA expression of TNF-α; it was expected due to an increase in the cAMP levels by Apremilast. The ability of SLNs to reduce the mRNA of TNF-α was expected due to the high internalization of the Apremilast compared to free Apremilast. The above-mentioned cell-

uptake study supports the enhanced uptake of Apremilast by SLNs, which facilitated improved efficacy by reducing inflammatory mediators.

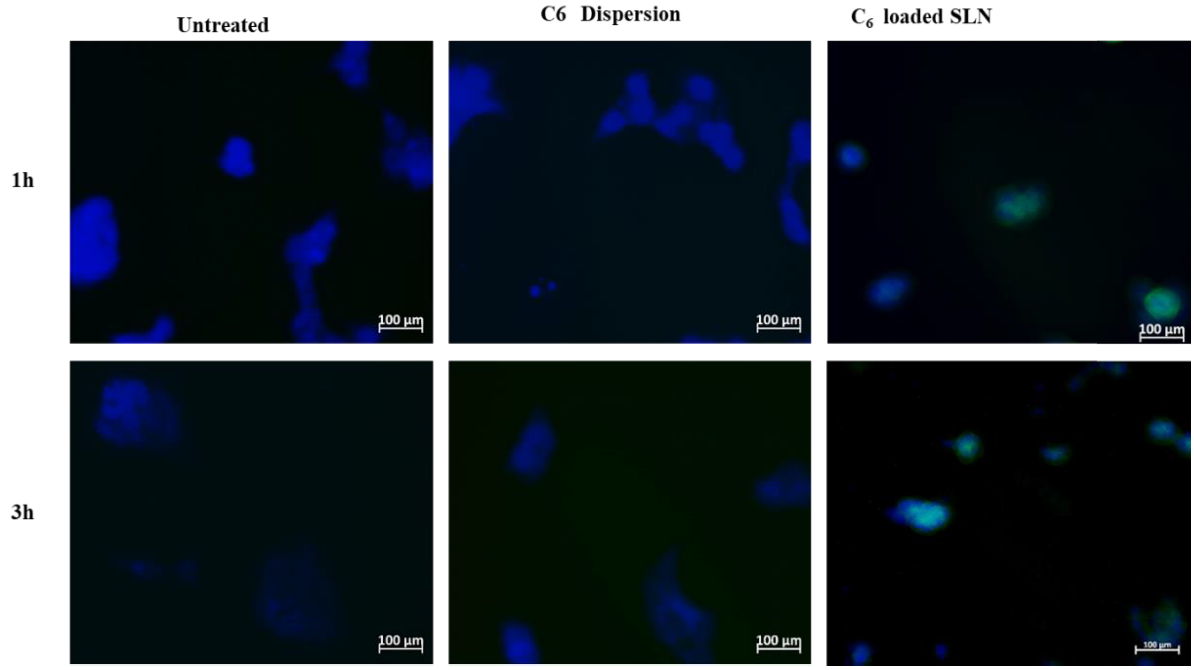


**Figure 3.10 A.** The Fluorescence microscopic images of cell uptake data.

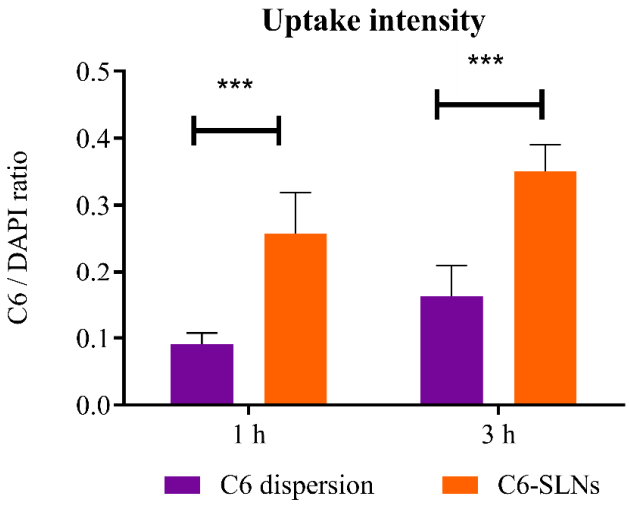


**Figure 3.10 B.** Cell uptake intensity of Coumarin-6 loaded SLNs and free Coumarin-6 (***p<0.0001).

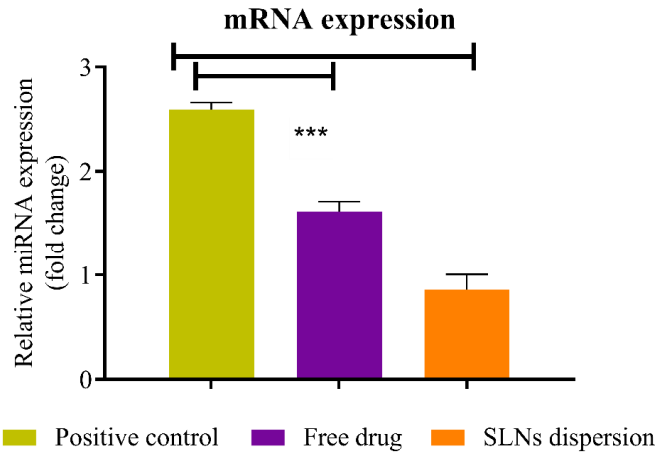


**Figure 3.11.** The relative reduction of TNF-α mRNA in imiquimod induced psoriasis model (n=3) (***p<0.0001).

### 3.3.9. Characterization of Apremilast loaded SLNs gel

Carbopol is a hydrophilic, high molecular weight, and crosslinked polyacrylic acid polymer. The Carbopol exhibits a tightly coiled structure in dry form. It is a weak anionic polymer it should be neutralized (basic pH) to achieve high pH. The polymer uncoils slightly on solvation (addition of water). The addition of appropriate amines (triethanolamine) and basic solution (sodium hydroxide solution) uncoil the Carbopol (neutralization) into the extended structure. The uncoiled system leads to rapid and extensive thickening of gel (crosslinking) [32].

#### 3.3.9.1. Rheological behavior

The gel was evaluated for viscosity, amplitude sweep test, and frequency sweep test using Anton Paar Rheometer with cone type (CP25) configuration with a 0.05 mm gap. The smaller gap height on the sample with constant shear was achieved due to the cone shape geometry. The rheological behavior graphs are represented in **Figure 3.12 (A-D)**. The viscosity of the prepared gel was found to be 6669 mPa.s at a constant shear rate, as depicted in **Figure 3.12 A.** An increase in time did not alter the Carbopol gel's viscosity, it was expected due to

Newtonian behavior. The Carbopol lingers fully structured due to the test's constant shear rate [32,33].

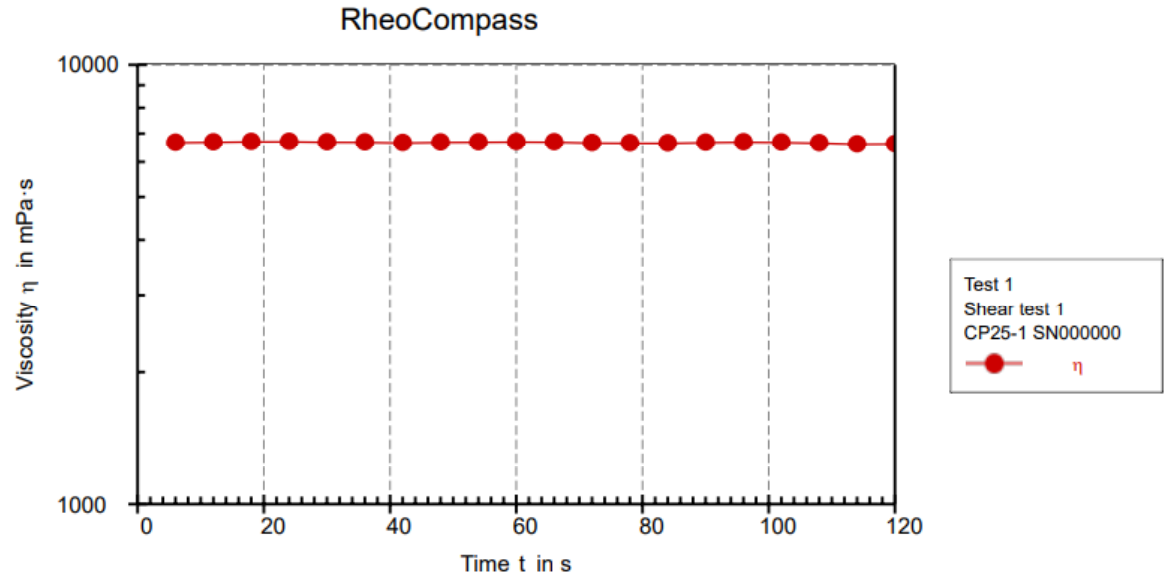


**Figure 3.12 A.** Viscosity of Apremilast loaded SLNs gel formulation with respect to time.

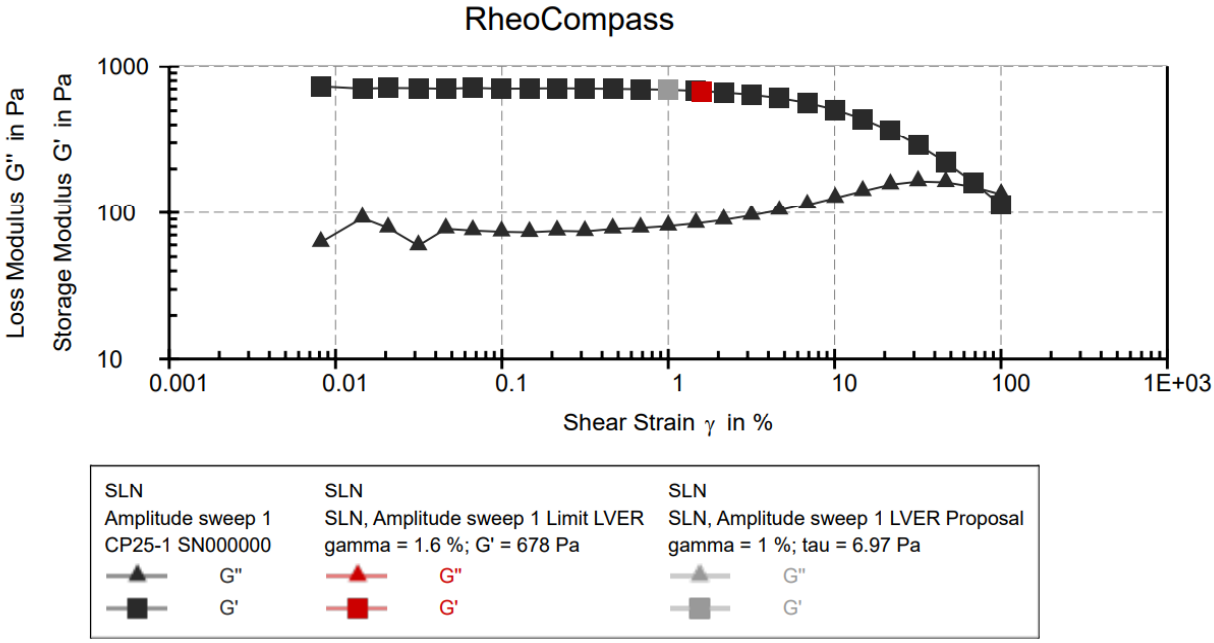


**Figure 3.12 B.** Amplitude sweep test of Apremilast loaded SLNs gel formulation employing angular frequency.

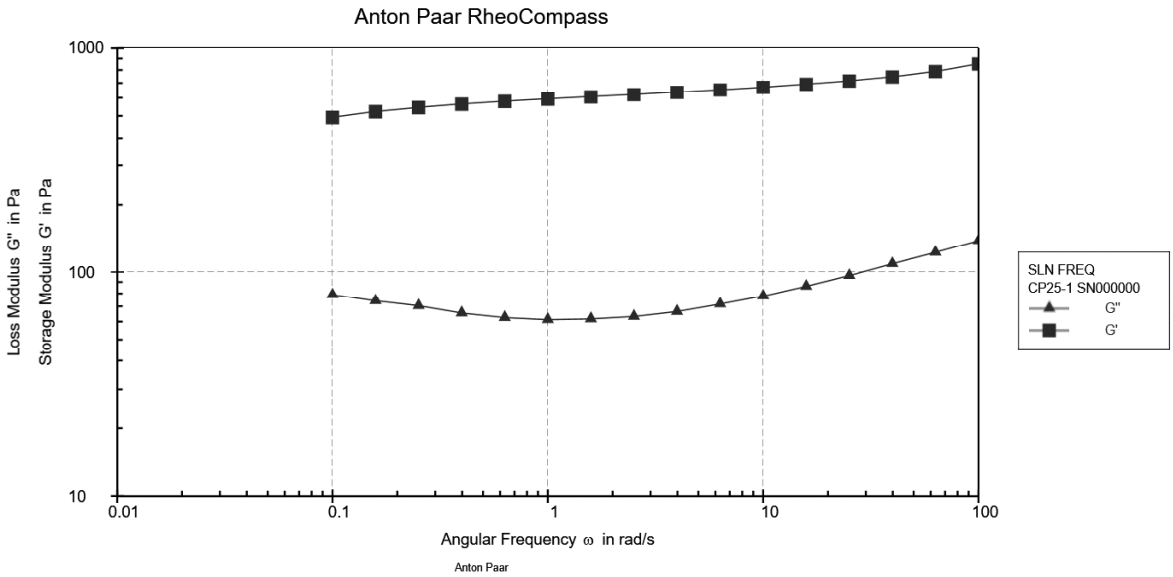


**Figure 3.12 C.** Frequency sweep test of Apremilast loaded SLNs gel formulation (loss modulus and storage modulus).

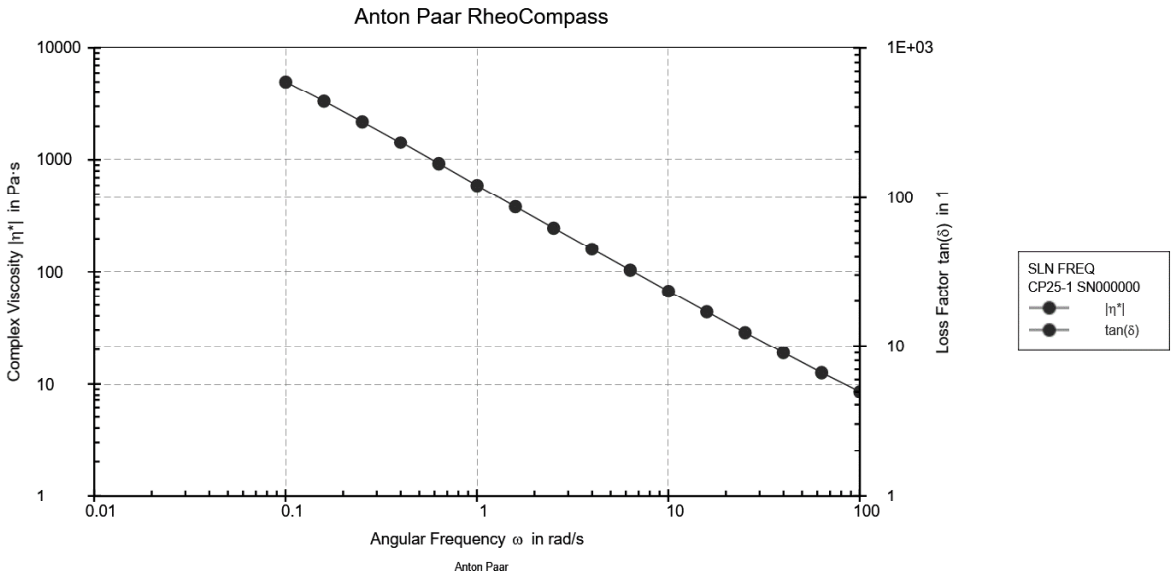


**Figure 3.12 D.** Frequency sweep test of Apremilast loaded SLNs gel formulation (Complex viscosity).

The amplitude sweep test exhibited the gel's linear viscoelastic behaviour and demonstrated solid-like properties at the lower strain. The results reveal the prepared gel can hold back maximum strain before structural deformation. The storage modulus was exhausted outside the critical strain 1.6%, as depicted in **Figure 3.12 B.** The frequency sweep test results revealed

that there was no change observed in storage modulus (G'), implying high stability of gel, which was expected due to an increase in structural strength and had a high degree of crosslinking as showed in **Figure 3.12 C and Figure 3.12 D**. The Apremilast loaded SLNs gel exhibited significantly higher storage modulus (G') compared to loss modulus (G"), indicating good structural stability [34,35].

#### 3.3.9.2. Occlusive Test

The formulation's ability to form an occlusive layer on the skin controls the percentage of TEWL. The results of the occlusion test are represented in **Figure 3.13 A**. The occlusive factor of SLNs loaded gel was 58.06 ± 0.420 and free drug-loaded gel was 8.302 ± 0.587 in 48 h. The results revealed that the Apremilast loaded SLNs gel reduced in percentage water loss through cellulose acetate membrane compared to free drug-loaded gel. The increased occlusive nature observed in the Apremilast loaded SLNs gel contributed by the formation of thin solid lipid layer on the cellulose acetate paper surface [20]. The high occlusion of SLNs (6.99 fold higher) favors improved permeation in the skin layers due to decreased TEWL.

#### 3.3.9.3. Ex-vivo studies

##### 3.3.9.3.1. Skin Permeation studies

The aliquots collected from the receptor compartment were analyzed for drug content. There was a non-detectable amount of drug for the first 6 h. The cumulative amount of drug permeated through the skin after 24 h was 3.97 ± 0.40% (n=3) from Apremilast loaded SLNs gel formulation, whereas 2.00 ± 0.06% from the free drug-loaded gel. The cumulative amount of drug permeated is represented in **Figure 3.13 B.** The SLNs formulation flux (0.293 $\mu g/h/cm^2$) was 1.72 fold higher compared to free drug formulation (0.169 $\mu g/h/cm^2$). The permeability coefficient of SLNs formulation and the free drug-loaded gel was $0.97\times10^{-3}$ and

$0.56\times10^{-3}$. The improved permeation of Apremilast loaded SLNs gel formulation was expected due to the occlusive nature and nano size of lipid nanocarriers.

#### 3.3.9.3.2. Dermal retention studies

The amount of drug retained in the skin was estimated by extracting the drug from the skin tissue. The drug retained in the skin was found to be 28.37 ± 1.18 µg/cm$^2$ and 12.39 ± 1.14 µg/cm$^2$ for Apremilast loaded SLNs gel and free drug-loaded gel respectively. The amount of drug retention in stratum corneum was 18.88 ± 1.18 µg/cm$^2$ and 9.49 ± 1.85 µg/cm$^2$ for Apremilast loaded SLNs gel. The amount of drug retention in stratum corneum was 8.85 ± 1.14 µg/cm$^2$ and 3.54 ± 1.06 µg/cm$^2$ for free drug-loaded gel (**Figure 3.13 C**). The drug permeated through the skin and determined in donor cells indicated the drug's transdermal delivery, whereas the drug retained in the skin represented the localized topical delivery. The low transdermal flux (0.293 µg/h/cm$^2$) and the permeation coefficient indicated low permeation and high skin retention. The reduction of TEWL results in the improved permeation of SLNs compared to free drug-loaded gel. The hydrogel imparts the additional hydrating effect to SLNs. The improved permeation and retention of drug, wherein the lipid vehicle played an vital role in generating alterations at cellular and physiological environment in a particular domain. In addition, effect may be imputed to formation of micro-reservoir of drug into the interiors of skin so as to affect its retention [36]. The results depicted the advantage of SLNs formulation for targeted delivery in the skin layers for effective psoriasis therapy. An increase in skin retention can minimize the unwanted adverse effects related to the drug.

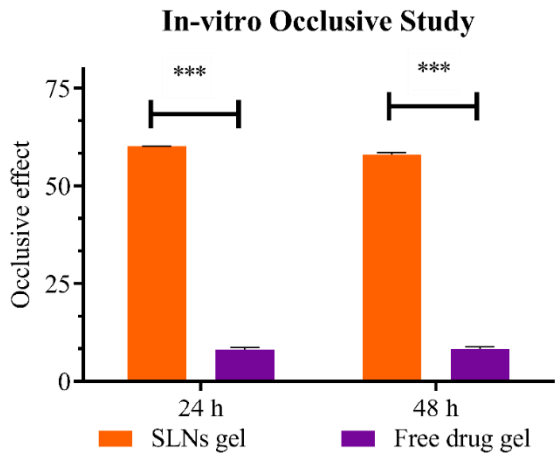


**Figure 3.13 A.** Occlusive effect of Apremilast loaded SLNs gel and free drug-loaded gel (Mean ± SD, n = 3) (***p<0.0001).

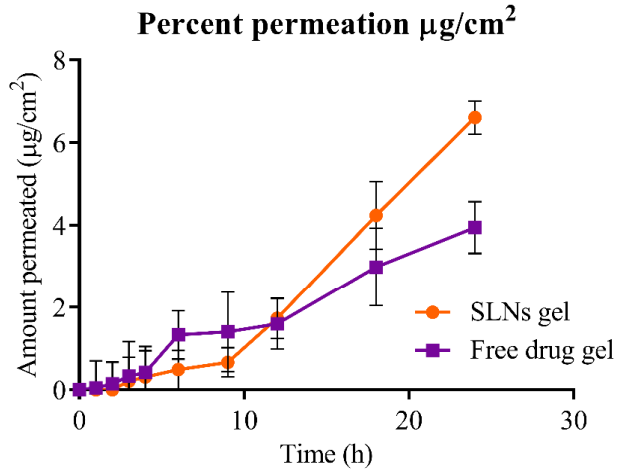


**Figure 3.13 B.** Ex-vivo skin permeation profiles of Apremilast loaded SLNs gel compared with free drug-loaded gel (Mean ± SD, n=3).

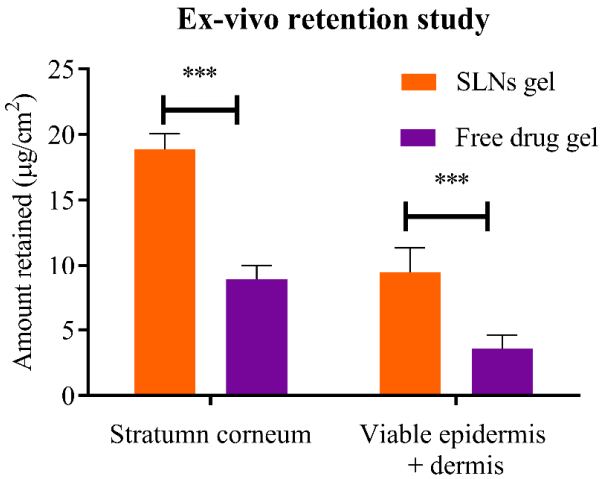


**Figure 3.13 C.** Skin retention study of Apremilast loaded SLNs gel compared with free drug-loaded gel (Mean ± SD, n=3) (***p<0.0001).

#### 3.3.9.3.3. Ex-vivo dermal distribution studies

The ex-vivo dermal distribution of Coumarin-6 aqueous dispersion and Coumarin-6 loaded SLNs formulation was performed to determine the drug distribution in different skin layers. Coumarin-6 is a poorly permeable compound into the skin. Thus, Coumarin-6 was selected as a dye to determine the drug distribution in skin layers. The results are depicted in **Figure 3.14** (Figure 3.14 A – Skin treated with free Coumarin-6 for 8 h; Figure 3.14 B – Skin treated with free Coumarin-6 for 16 h; Figure 3.14 C – Skin treated with Coumarin-6 loaded SLNs for 8 h; and Figure 3.14 D – Skin treated with Coumarin-6 loaded SLNs for 16 h). The study confirms the low permeation of free Coumarin-6 visible as a green fluorescence only on superficial skin layers (after 8 h and 16 h). The distribution of Coumarin-6 loaded SLNs depicted high intensity of dye in the stratum corneum at 8 h study. Then after 16 h, there was a marginal distribution into the deeper layers of skin. The study reflected the permeation of designed SLNs into deeper layers by diffusion through the stratum corneum and confined to the root of hair follicles. The results confirmed that the optimized SLNs composition could improve the permeation and skin retention, as observed in the ex-vivo study. It was expected due to the nanosize of the SLNs ascribed to accumulation in hair follicles and deeper layers. The results represented that the prepared SLNs can improve permeation and skin retention of the Apremilast.

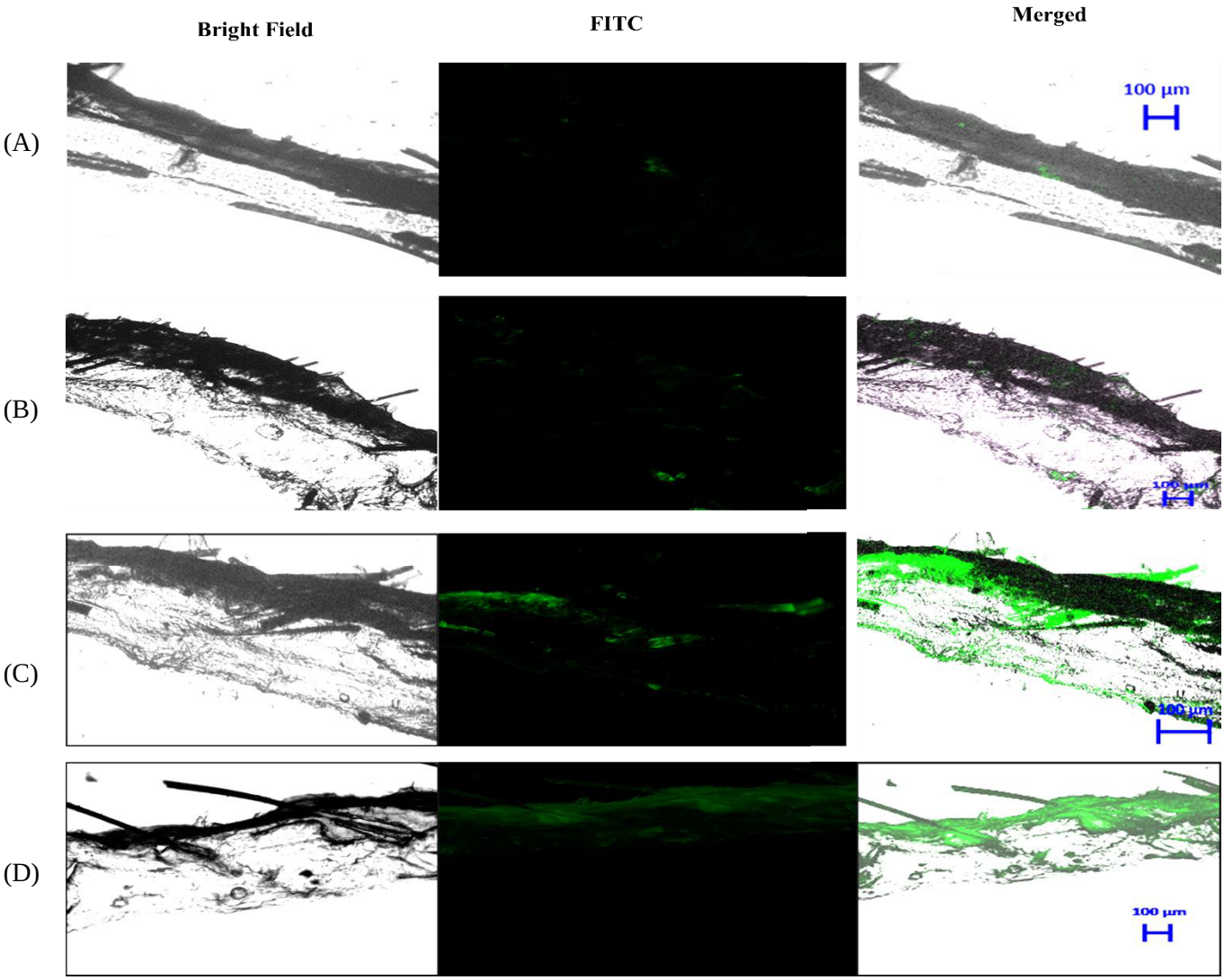


**Figure 3.14 A.** Skin treated with free Coumarin-6 for 8 h; **Figure 3.14 B.** Skin treated with free Coumarin-6 for 16 h; **Figure 3.14 C.** Skin treated with Coumarin-6 loaded SLNs for 8 h; **Figure 3.14 D.** Skin treated with Coumarin-6 loaded SLNs for 16 h.

### 3.3.9.3.4. Dermatokinetic estimation

The dermatokinetic profile of the Apremilast loaded SLNs gel and free drug-loaded gel in the epidermis and dermis is represented in **Figures 3.15 A and Figure 3.15 B**. The drug retention with SLNs formulation was 2 fold higher in the epidermis and 5 fold higher in the dermis than free drug-loaded gel (***$p<0.0001$). The $C_{maxSkin}$ of the Apremilast loaded SLNs gel and free drug-loaded gel in epidermis were found to be 98.311 ± 2.121 µg/cm$^2$ and 41.768 ± 2.518

µg/cm$^2$ respectively. In dermis, the $C_{maxSkin}$ of the Apremilast loaded SLNs gel and free drug-loaded gel were found to be 68.686 ± 5.657 µg/cm$^2$ and 13.047 ± 3.107 µg/cm$^2$ respectively. The $T_{max}$ of both the formulations were found similar 6.00 h in the epidermis and 8.00 h in the dermis. The $AUC_{0–24}$ of the Apremilast-loaded SLNs gel was 3.33 fold higher in epidermis (1082.813 ± 80.610 µg/cm$^2$.h) compared to free drug-loaded gel (324.840 ± 8.828µg/cm$^2$.h). Whereas in dermis Apremilast-loaded SLNs gel showed 5.25 fold higher (1074.629 ± 137.553 µg/cm$^2$.h) compared to free drug-loaded gel (204.343 ± 8.482 µg/cm$^2$.h). The pharmacokinetic parameters of Apremilast loaded SLNs gel, and free drug-loaded gel are mentioned in **Table 3.10**.

**Table 3.10.** Summary of dermatokinetic evaluation of Apremilast loaded SLNs gel and free drug-loaded gel (n=4).

| **Parameter** | **Apremilast loaded SLNs gel** | | **Free drug-loaded gel** | |
|---|---|---|---|---|
| | **Epidermis** | **Dermis** | **Epidermis** | **Dermis** |
| **$AUC_{0–24}$ (µg/cm$^2$.h)** | 1082.812 ± 80.610 | 1074.629 ± 137.553 | 324.840 ± 8.828 | 204.343 ± 8.482 |
| **$AUC_{0\text{-}inf}$ (µg/cm$^2$.h)** | 1138.253 ± 92.648 | 2045.064 ± 246.963 | 465.389 ± 7.100 | 442.657 ± 62.786 |
| **$C_{maxSkin}$ (µg/cm$^2$)** | 98.311 ± 2.121 | 68.685 ± 5.657 | 41.768 ± 2.518 | 13.047 ± 3.107 |
| **$T_{max}$ (h)** | 6.000 | 8.000 | 6.000 | 8.000 |
| **$K_e$ (h$^{-1}$)** | 0.152 ± 0.011 | 0.037 ± 0.004 | 0.052 ± 0.001 | 0.030 ± 0.010 |

The study assured improved permeation and retention of Apremilast loaded SLNs gel. The nanosize and lipid constituents used in SLNs interact with skin attributing permeation into skin layers. A higher concentration in the epidermis is expected due to the embedding of SLNs in stratum corneum layers. The polar head group and non-polar chain of lipid helps in spontaneous structuring into skin layers. This favours interaction of formulation lipid and skin lipids and synergistically results in skin retention providing long last effect. The drug is expected to

embed in the stratum corneum (epidermis) and diffuse into deeper layers (dermis), which was depicted by the increase in the $T_{max}$ in dermis layers. The bio adhesiveness of the gel formulation may favors a high concentration of the drug in the epidermis layers in both formulations [37].

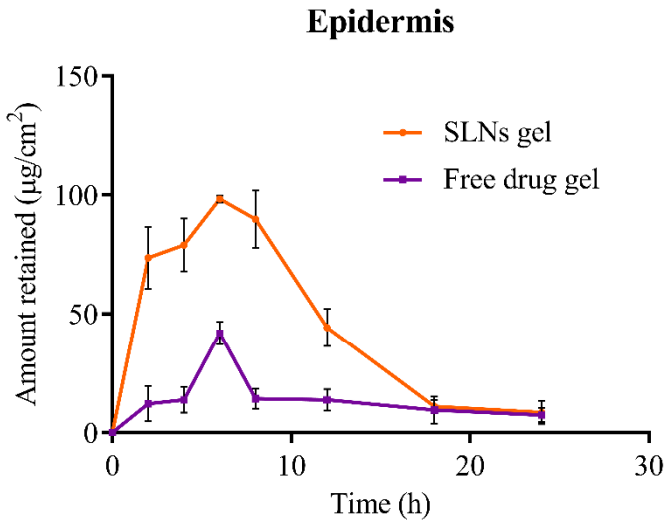


**Figure 3.15 A.** Dermatokinetic profile of Apremilast loaded SLNs gel compared with free drug-loaded gel in the epidermis (Mean ± SD, n=4) (***p<0.0001).

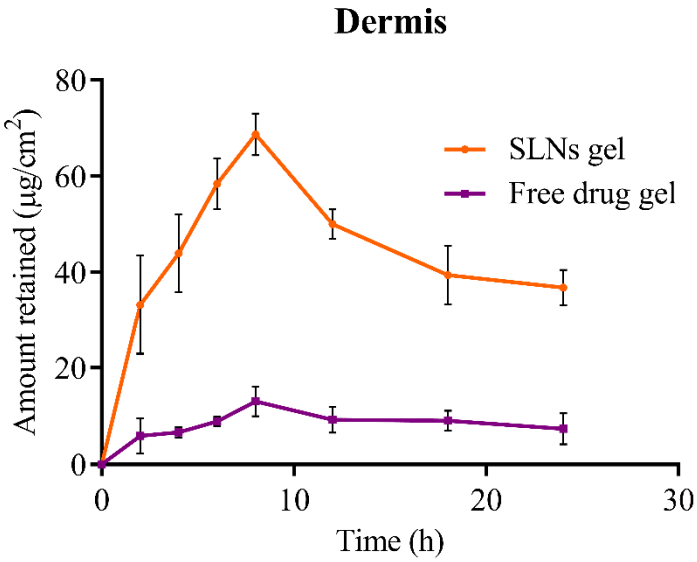


**Figure 3.15 B.** Dermatokinetic profile of Apremilast loaded SLNs gel compared with free drug-loaded gel in the dermis (Mean ± SD, n=4) (***p<0.0001).

### 3.3.10. In-vivo skin retention and irritation studies

The amount of drug retained (µg/cm$^2$) in skin layers of swiss albino mice treated with Apremilast loaded SLNs gel and free drug-loaded gel after 12 h and 24 h are illustrated in **Figure 3.16**. The amount of drug retained in the skin was higher in SLNs loaded gel formulation (3.53 fold in 12 h, 2.32 fold higher in 24 h) than free drug-loaded gel. The drug retained in the stratum corneum and viable part of the skin treated with Apremilast loaded SLNs gel, and free drug-loaded gel are represented in **Table 3.11.**

**Table 3.11.** Amount of Apremilast retained in the skin layers

| **Formulation** | | **Skin layers** | |
|---|---|---|---|
| | | **Stratum Corneum (µg/cm$^2$)** | **Viable epidermis + dermis (µg/cm$^2$)** |
| **SLNs gel** | **12 h** | 10.91 ± 1.75 | 4.00 ± 1.29 |
| | **24 h** | 5.44 ± 1.30 | 2.63 ± 0.75 |
| **Free drug loaded gel** | **12 h** | 2.16 ± 0.60 | 2.06 ± 0.56 |
| | **24 h** | 1.62 ± 0.85 | 1.85 ± 0.82 |

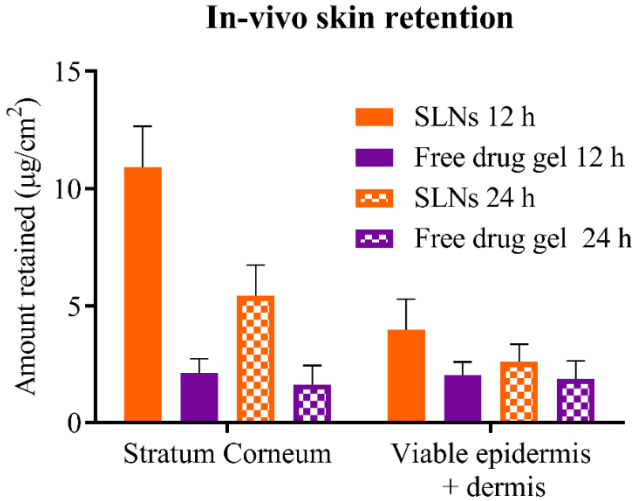


**Figure 3.16.** Skin retention of Apremilast in swiss albino mice treated with SLNs loaded gel and free drug-loaded gel for 12 h and 24 h.

The data revealed a high drug concentration in 12 h compared to 24 h in animals treated with Apremilast-loaded SLNs gel. As the data obtained in the dermatokinetic study, $T_{max}$ achieved

was 8 h, indicating a higher drug concentration in 12h compared to 24 h. The amount of drug retained was higher in Apremilast loaded SLNs gel compared to free drug preparation. The amount of drug in the stratum corneum after 12 h was similar in three formulations. The drug retained in skin layers up to 24 h indicates that the developed formulation can exhibit prolonged retention in skin layers [23,25]. The skin irritation studies showed no signs of irritation (inflammation and erythema) on the skin in 12h and 24h after applying the gel, as illustrated in **Figure 3.17**. The skin histology study showed that there were no signs of inflammation or changes in the skin. The H&E staining histology data is represented in **Figure 3.18**. The data showed the skin structure was intact and normal [26,27]. The results indicate the developed formulation is safe for topical delivery of Apremilast.

### 3.3.11. Storage stability of Apremilast loaded SLNs gel

The Apremilast-loaded SLNs gel was evaluated for stability up to three months. The hydrogel stability samples redispersed in water showed nanocarriers' integrity using Malvern zeta sizer without any aggregation (176.65 – 189.90 nm). The assay results (98.82 – 100.00 %) showed that there was no substantial change (< 2%) in drug content which indicating the stability of designed SLNs gel preparation. The stability data is depicted in **Table 3.12** [38].

**Table 3.12.** Stability data of Apremilast loaded SLNs gel (n=3).

| **Stability data of SLN dispersion loaded gel at 4** ℃ | | | | |
|---|---|---|---|---|
| **Parameter** | **0 Month** | **1 Month** | **2 Month** | **3 Month** |
| **Assay of gel (%)** | 100.00 ± 0.282 | 99.82 ± 0.353 | 99.75 ± 0.282 | 99.58 ± 0.424 |
| **Size (nm)** | 176.65 ± 1.767 | 182.45 ± 3.041 | 187.60 ± 2.687 | 189.15 ± 0.106 |
| **PDI** | 0.244 ± 0.013 | 0.261 ± 0.007 | 0.283 ± 0.040 | 0.272 ± 0.023 |
| **Stability data of SLN dispersion loaded gel at 25** ℃ | | | | |
| **Assay of gel (%)** | 100.00 ± 0.282 | 99.41 ± 0.254 | 98.90 ± 0.347 | 98.82 ± 0.219 |
| **Size (nm)** | 176.65 ± 1.767 | 188.40 ± 2.194 | 189.51 ± 3.689 | 189.90 ± 3.162 |
| **PDI** | 0.244 ± 0.013 | 0.258 ± 0.016 | 0.287 ± 0.033 | 0.311 ± 0.0419 |

| Formulation | Before application of gel | After application of gel |
| --- | --- | --- |
| SLNs loaded gel | 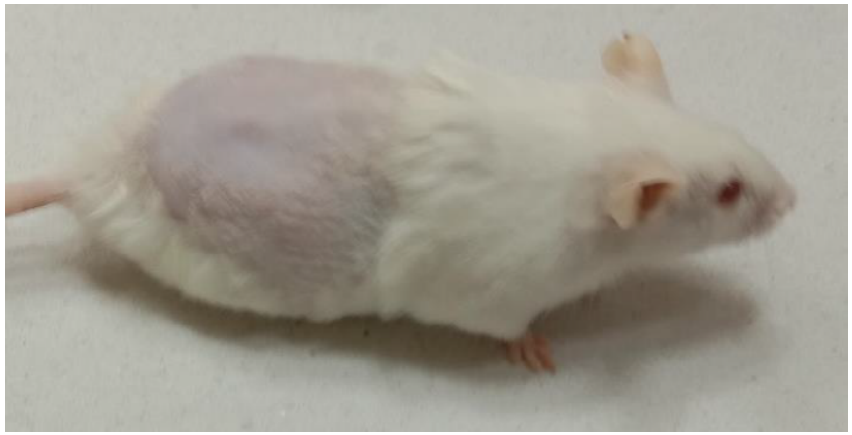 | 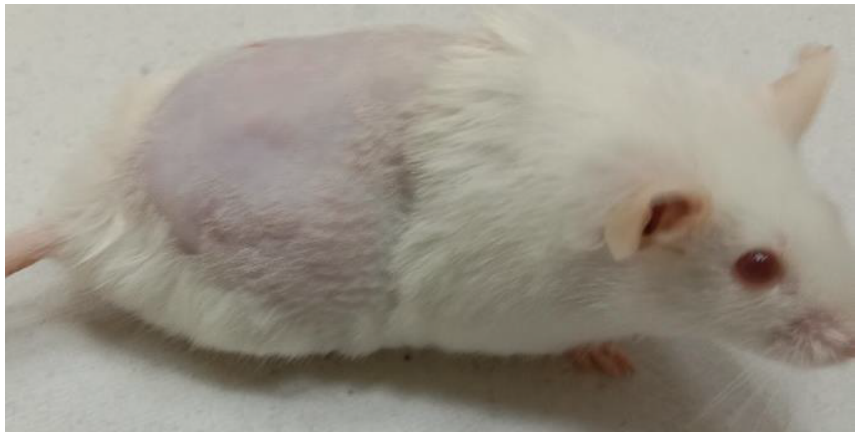 |
| Free drug-loaded gel | 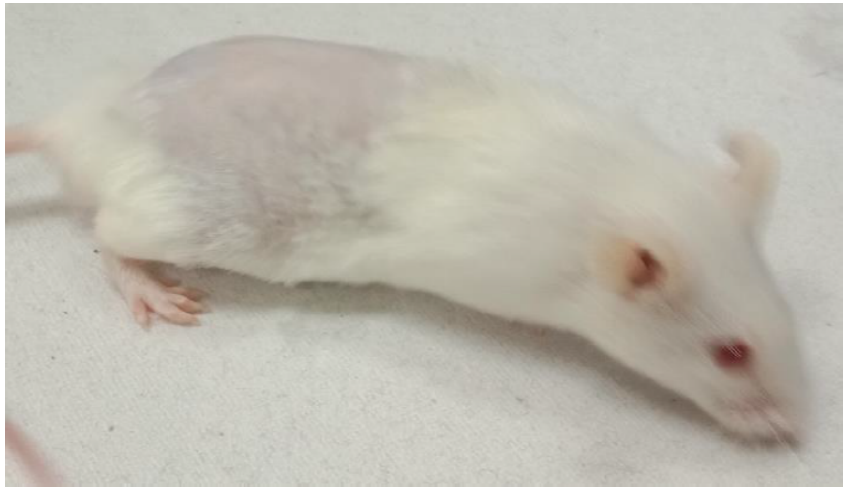 | 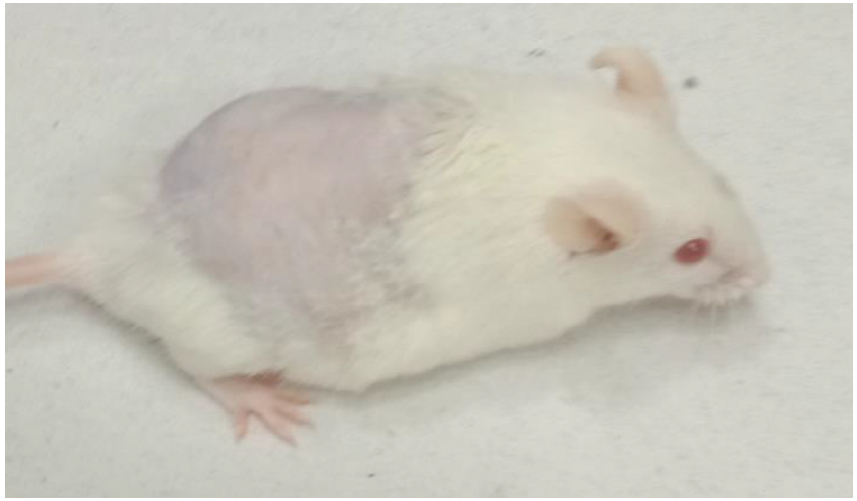 |

**Figure 3.17** The animal images for signs of irritation (inflammation and erythema) after and before application.

| Formulation | 12 h | 24 h |
| --- | --- | --- |
| SLNs loaded gel | 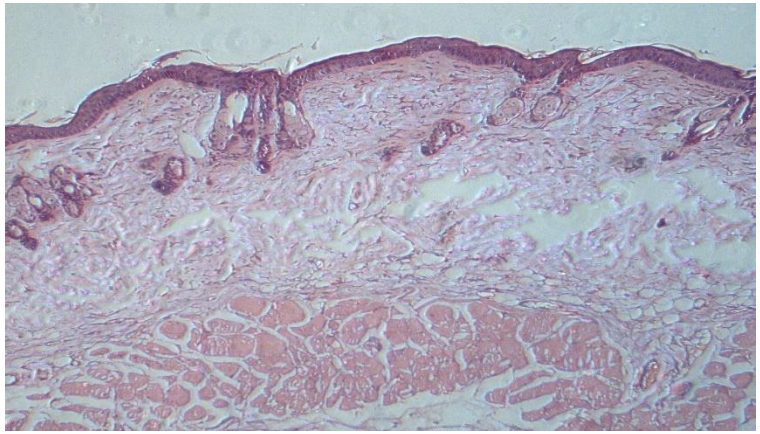 | 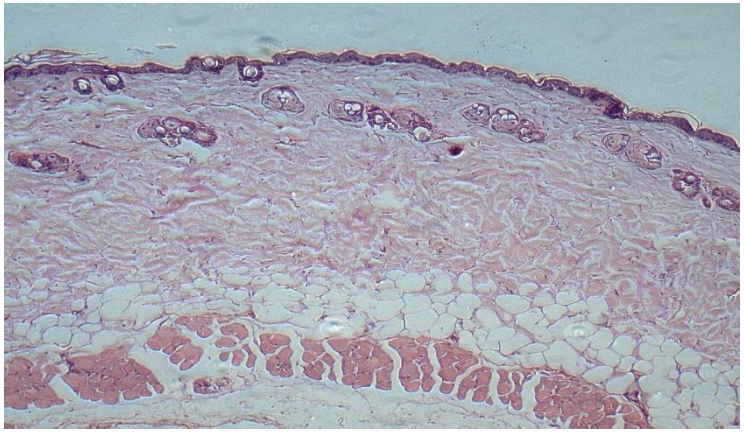 |
| Free drug-loaded gel | 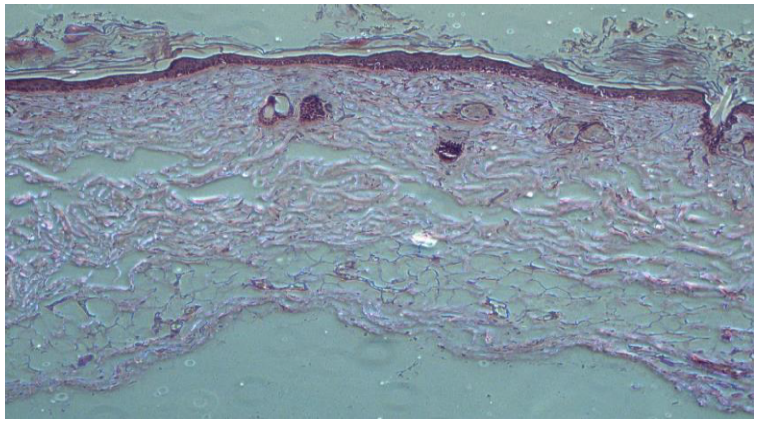 | 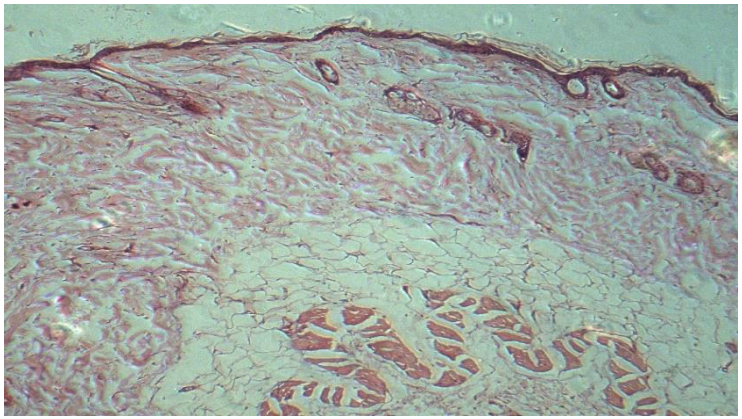 |

**Control (without application of formulation)**

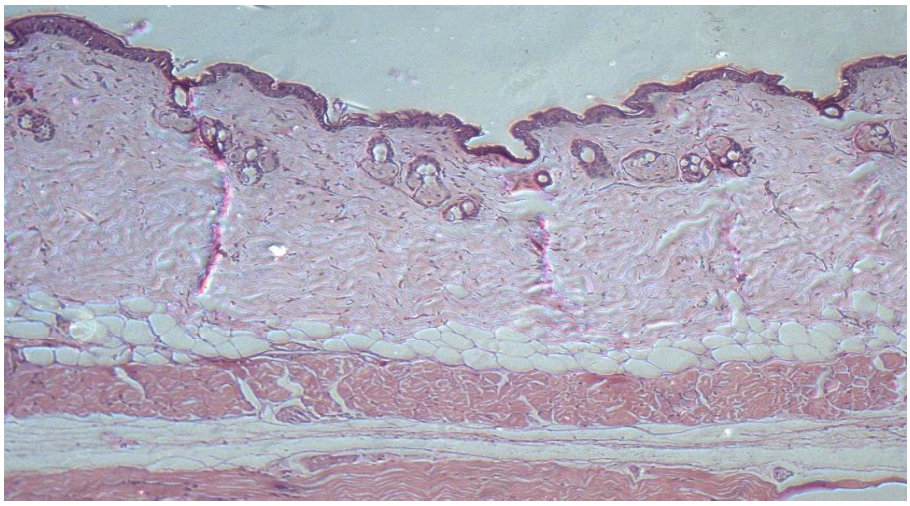

**Figure 3.18.** The H&E staining histology data after 12 h and 24 h of application

### 3.4. Conclusion

Apremilast loaded SLNs were developed by applying the QbD approach, and its potential increase in skin permeation and retention was determined. Box Behnken design was employed, and the effect of amount of lipid, surfactant concentration and sonication time on particle size and entrapment efficiency were determined. The results demonstrated that the topical Apremilast delivery by SLNs enhanced skin permeation and retention, which was expected due to the occlusive effect by forming a thin layer. The in vitro release studies revealed extended drug release from SLN dispersion. The in vitro cell line studies reflected the safety of the formulation excipients, and the reduction of TNF-α messenger Ribonucleic acid (mRNA) levels indicated the SLNs formulation's efficacy. The skin retention study and dermatokinetic study depicted the enhanced concentration in skin layers, suggesting the skin layers targeting ability with minimizing the systemic absorption. The in-vivo studies performed on swiss albino mice represented the higher concentration in skin layers with Apremilast loaded SLNs gel. The concentration was reduced with an increase in time, although indicating the prolonged retention in skin layers.

## References


[1] T.P. Afra, T.M. Razmi, S. Dogra, Apremilast in Psoriasis and Beyond: Big Hopes on a Small Molecule., Indian Dermatol. Online J. 10 (2019) 1–12. https://doi.org/10.4103/idoj.IDOJ_437_18.

[2] K. Papp, K. Reich, C.L. Leonardi, L. Kircik, S. Chimenti, R.G.B. Langley, C.C. Hu, R.M. Stevens, R.M. Day, K.B. Gordon, N.J. Korman, C.E.M. Griffiths, Apremilast, an oral phosphodiesterase 4 (PDE4) inhibitor, in patients with moderate to severe plaque psoriasis: Results of a phase III, randomized, controlled trial (Efficacy and Safety Trial Evaluating the Effects of Apremilast in Psoriasis [ESTEEM] 1), J. Am. Acad. Dermatol. 73 (2015) 37–49. https://doi.org/10.1016/j.jaad.2015.03.049.

[3] T.P. Afra, T.M. Razmi, S. Dogra, Apremilast in Psoriasis and Beyond: Big Hopes on a Small Molecule., Indian Dermatol. Online J. 10 (2019) 1–12. https://doi.org/10.4103/idoj.IDOJ_437_18.

[4] R. Kumar, S. Dogra, B. Amarji, B. Singh, S. Kumar, Sharma, K. Vinay, R. Mahajan, O.P. Katare, Efficacy of Novel Topical Liposomal Formulation of Cyclosporine in Mild to Moderate Stable Plaque Psoriasis, JAMA Dermatology. 152 (2016) 807. https://doi.org/10.1001/jamadermatol.2016.0859.

[5] V.K. Rapalli, G. Singhvi, S.K. Dubey, G. Gupta, D.K. Chellappan, K. Dua, Emerging landscape in psoriasis management: From topical application to targeting biomolecules, Biomed. Pharmacother. 106 (2018) 707–713. https://doi.org/10.1016/j.biopha.2018.06.136.

[6] V.A. Duong, T.T.L. Nguyen, H.J. Maeng, Preparation of solid lipid nanoparticles and nanostructured lipid carriers for drug delivery and the effects of preparation parameters of solvent injection method, Molecules. 25 (2020) 1–36. https://doi.org/10.3390/molecules25204781.

[7] Y. Duan, A. Dhar, C. Patel, M. Khimani, S. Neogi, P. Sharma, N. Siva Kumar, R.L. Vekariya, A brief review on solid lipid nanoparticles: Part and parcel of contemporary drug delivery systems, RSC Adv. 10 (2020) 26777–26791. https://doi.org/10.1039/d0ra03491f.

[8] V.K. Rapalli, V. Kaul, T. Waghule, S. Gorantla, S. Sharma, A. Roy, S.K. Dubey, G.

Singhvi, Curcumin loaded nanostructured lipid carriers for enhanced skin retained topical delivery: optimization, scale-up, in-vitro characterization and assessment of ex-vivo skin deposition, Eur. J. Pharm. Sci. 152 (2020) 105438. https://doi.org/10.1016/j.ejps.2020.105438.

[9] A. Mahmood, V.K. Rapalli, T. Waghule, S. Gorantla, G. Singhvi, Luliconazole loaded lyotropic liquid crystalline nanoparticles for topical delivery: QbD driven optimization, in-vitro characterization and dermatokinetic assessment, Chem. Phys. Lipids. 234 (2021) 105028. https://doi.org/10.1016/j.chemphyslip.2020.105028.

[10] V.K. Rapalli, S. Banerjee, S. Khan, P.N. Jha, G. Gupta, K. Dua, M.S. Hasnain, A.K. Nayak, S.K. Dubey, G. Singhvi, QbD-driven formulation development and evaluation of topical hydrogel containing ketoconazole loaded cubosomes, Mater. Sci. Eng. C. (2020) 111548. https://doi.org/10.1016/j.msec.2020.111548.

[11] V.K. Rapalli, A. Khosa, G. Singhvi, V. Girdhar, R. Jain, S.K. Dubey, Application of QbD Principles in Nanocarrier-Based Drug Delivery Systems, Pharm. Qual. by Des. (2019) 255–296. https://doi.org/10.1016/B978-0-12-815799-2.00014-9.

[12] M.K. Chauhan, P.K. Sharma, Optimization and characterization of rivastigmine nanolipid carrier loaded transdermal patches for the treatment of dementia, Chem. Phys. Lipids. 224 (2019). https://doi.org/10.1016/j.chemphyslip.2019.104794.

[13] T. Waghule, V.K. Rapalli, G. Singhvi, P. Manchanda, N. Hans, S.K. Dubey, M.S. Hasnain, A.K. Nayak, Voriconazole loaded nanostructured lipid carriers based topical delivery system: QbD based designing, characterization, in-vitro and ex-vivo evaluation, J. Drug Deliv. Sci. Technol. 52 (2019) 303–315. https://doi.org/10.1016/j.jddst.2019.04.026.

[14] A. Mahmood, V.K. Rapalli, T. Waghule, S. Gorantla, S.K. Dubey, R.N. Saha, G. Singhvi, UV spectrophotometric method for simultaneous estimation of betamethasone valerate and tazarotene with absorption factor method: Application for in-vitro and ex-vivo characterization of lipidic nanocarriers for topical delivery, Spectrochim. Acta - Part A Mol. Biomol. Spectrosc. 235 (2020) 118310. https://doi.org/10.1016/j.saa.2020.118310.

[15] S.R. Varma, T.O. Sivaprakasam, A. Mishra, S. Prabhu, M. Rafiq, P. Rangesh, Imiquimod-induced psoriasis-like inflammation in differentiated Human keratinocytes:

Its evaluation using curcumin, Eur. J. Pharmacol. 813 (2017) 33–41. https://doi.org/10.1016/j.ejphar.2017.07.040.

[16] N. Shraibom, A. Madaan, V. Joshi, R. Verma, A. Chaudhary, G. Mishra, A. Awasthi, A.T. Singh, M. Jaggi, Evaluation of in vitro Anti-psoriatic Activity of a Novel Polyherbal Formulation by Multiparametric Analysis, Antiinflamm. Antiallergy. Agents Med. Chem. 16 (2017). https://doi.org/10.2174/1871523016666170720160037.

[17] R. Arora, S.S. Katiyar, V. Kushwah, S. Jain, Solid lipid nanoparticles and nanostructured lipid carrier-based nanotherapeutics in treatment of psoriasis: a comparative study, Expert Opin. Drug Deliv. 14 (2017) 165–177. https://doi.org/10.1080/17425247.2017.1264386.

[18] P.R. Wavikar, P.R. Vavia, Rivastigmine-loaded in situ gelling nanostructured lipid carriers for nose to brain delivery, J. Liposome Res. 25 (2015) 141–149. https://doi.org/10.3109/08982104.2014.954129.

[19] M. Ahirrao, S. Shrotriya, In vitro and in vivo evaluation of cubosomal in situ nasal gel containing resveratrol for brain targeting, Drug Dev. Ind. Pharm. 43 (2017) 1686–1693. https://doi.org/10.1080/03639045.2017.1338721.

[20] V. Kakkar, I.P. Kaur, A.P. Kaur, K. Saini, K.K. Singh, Topical delivery of tetrahydrocurcumin lipid nanoparticles effectively inhibits skin inflammation: in vitro and in vivo study, Drug Dev. Ind. Pharm. 44 (2018) 1701–1712. https://doi.org/10.1080/03639045.2018.1492607.

[21] H. Badie, H. Abbas, Novel small self-assembled resveratrol-bearing cubosomes and hexosomes: preparation, charachterization, and ex vivo permeation, Drug Dev. Ind. Pharm. 44 (2018) 2013–2025. https://doi.org/10.1080/03639045.2018.1508220.

[22] P. Verma, M. Ahuja, Cubic liquid crystalline nanoparticles: optimization and evaluation for ocular delivery of tropicamide, Drug Deliv. 23 (2016) 3043–3054. https://doi.org/10.3109/10717544.2016.1143057.

[23] R. Sonawane, H. Harde, M. Katariya, S. Agrawal, S. Jain, Solid lipid nanoparticles-loaded topical gel containing combination drugs: An approach to offset psoriasis, Expert Opin. Drug Deliv. 11 (2014) 1833–1847. https://doi.org/10.1517/17425247.2014.938634.

[24] N. Thotakura, P. Kumar, S. Wadhwa, K. Raza, P. Katare, Dermatokinetics as an Important Tool to Assess the Bioavailability of Drugs by Topical Nanocarriers, Curr. Drug Metab. 18 (2017) 404–411. https://doi.org/10.2174/1389200218666170306104042.

[25] P.M. Al-Maghrabi, E.S. Khafagy, M.M. Ghorab, S. Gad, Influence of formulation variables on miconazole nitrate–loaded lipid based nanocarrier for topical delivery, Colloids Surfaces B Biointerfaces. 193 (2020) 111046. https://doi.org/10.1016/j.colsurfb.2020.111046.

[26] J. Sun, W. Dou, Y. Zhao, J. Hu, A comparison of the effects of topical treatment of calcipotriol, camptothecin, clobetasol and tazarotene on an imiquimod-induced psoriasis-like mouse model, Immunopharmacol. Immunotoxicol. 36 (2014) 17–24. https://doi.org/10.3109/08923973.2013.862542.

[27] A. Dadwal, N. Mishra, R.K. Rawal, R.K. Narang, Development and characterisation of clobetasol propionate loaded Squarticles as a lipid nanocarrier for treatment of plaque psoriasis, J. Microencapsul. (2020) 1–14. https://doi.org/10.1080/02652048.2020.1756970.

[28] T. Waghule, V.K. Rapalli, S. Gorantla, R.N. Saha, S.K. Dubey, A. Puri, G. Singhvi, Nanostructured Lipid Carriers as Potential Drug Delivery Systems for Skin disorders, Curr. Pharm. Des. 26 (2020). https://doi.org/10.2174/1381612826666200614175236.

[29] G. Schett, V.S. Sloan, R.M. Stevens, P. Schafer, Apremilast: A novel PDE4 inhibitor in the treatment of autoimmune and inflammatory diseases, Ther. Adv. Musculoskelet. Dis. 2 (2010) 271–278. https://doi.org/10.1177/1759720X10381432.

[30] H. Yuan, J. Miao, Y.Z. Du, J. You, F.Q. Hu, S. Zeng, Cellular uptake of solid lipid nanoparticles and cytotoxicity of encapsulated paclitaxel in A549 cancer cells, Int. J. Pharm. 348 (2008) 137–145. https://doi.org/10.1016/j.ijpharm.2007.07.012.

[31] H. Sumida, K. Yanagida, Y. Kita, J. Abe, K. Matsushima, M. Nakamura, S. Ishii, S. Sato, T. Shimizu, Interplay between CXCR2 and BLT1 Facilitates Neutrophil Infiltration and Resultant Keratinocyte Activation in a Murine Model of Imiquimod-Induced Psoriasis, J. Immunol. 192 (2014) 4361–4369. https://doi.org/10.4049/jimmunol.1302959.

[32] P. R. Varges, C. M. Costa, B. S. Fonseca, M. F. Naccache, P. De Souza Mendes, Rheological Characterization of Carbopol® Dispersions in Water and in Water/Glycerol Solutions, Fluids. 4 (2019) 3. https://doi.org/10.3390/fluids4010003.

[33] C. Gazga-Urioste, E. Rivera-Becerril, G. Pérez-Hernández, N. Angélica Noguez-Méndez, A. Faustino-Vega, C. Tomás Quirino-Barreda, Physicochemical characterization and thermal behavior of hexosomes containing ketoconazole as potential topical antifungal delivery system, Drug Dev. Ind. Pharm. 45 (2019) 168–176. https://doi.org/10.1080/03639045.2018.1526188.

[34] L.Q. Ying, M. Misran, Rheological and physicochemical characterization of alpha-tocopherol loaded lipid nanoparticles in thermoresponsive gel for topical application, Malaysian J. Fundam. Appl. Sci. 13 (2017) 248–252. https://doi.org/10.11113/mjfas.v13n3.596.

[35] J. Simta, I. Kavita, B. Milind, Novel Long Retentive Posaconazole Ophthalmic Suspension, 6 (2020) 1–10. https://doi.org/10.11648/j.pst.20200401.11.

[36] N.K. Garg, G. Sharma, B. Singh, P. Nirbhavane, R.K. Tyagi, R. Shukla, O.P. Katare, Quality by Design (QbD)-enabled development of aceclofenac loaded-nano structured lipid carriers (NLCs): An improved dermatokinetic profile for inflammatory disorder(s), Int. J. Pharm. 517 (2017) 413–431. https://doi.org/10.1016/J.IJPHARM.2016.12.010.

[37] M.S. Freag, A.S. Torky, M.M. Nasra, D.A. Abdelmonsif, O.Y. Abdallah, Liquid crystalline nanoreservoir releasing a highly skin-penetrating berberine oleate complex for psoriasis management, Nanomedicine. 14 (2019) 931–954. https://doi.org/10.2217/nnm-2018-0345.

[38] V.A. Guilherme, L.N.M. Ribeiro, A.C.S. Alcântara, S.R. Castro, G.H. Rodrigues da Silva, C.G. da Silva, M.C. Breitkreitz, J. Clemente-Napimoga, C.G. Macedo, H.B. Abdalla, R. Bonfante, C.M.S. Cereda, E. de Paula, Improved efficacy of naproxen-loaded NLC for temporomandibular joint administration, Sci. Rep. 9 (2019) 1–11. https://doi.org/10.1038/s41598-019-47486-w.